SCALING AND FUNCTION OF SPIDER SAFETY LINE

by

CHRISTINE SILKE ORTLEPP

B. Sc., The University of British Columbia, 1995

A THESIS SUBMITTED IN PARTIAL FULFILLMENT OF
THE REQUIREMENTS FOR THE DEGREE OF

MASTER OF SCIENCE

in

THE FACULTY OF GRADUATE STUDIES

(Department of Zoology)

THE UNIVERSITY OF BRITISH COLUMBIA

December 2001

© Christine Silke Ortlepp, 2001

Chapter 1: Introduction

Over the more than 380 million years that spiders have roamed the Earth (Sheldon et al., 1991), as many as nine different types of silk have evolved of which up to seven can be found in any one species. Different types of silk are made by different glands in the abdomen, have different mechanical properties and are used for different purposes. Some functions include safety lines, web construction, glue, wrapping prey, protecting eggs, transferring sperm, building retreats, communication and locomotion (Foelix, 1996).

Some kinds of silk, like viscid silk, have a single function and have material properties that are closely matched to that use. Viscid silk forms the sticky capture spiral in the orb webs of ecribbilate spiders and is made up of the products from two glands; a pair of fibres made by the flagelliform gland, and a sticky viscous coating from the aggregate gland. Together they form a material that appears to be perfectly adapted to its function of capturing aerial prey with low stiffness, very high extension and excellent energy dissipation (Gosline et al., 1986).

Other silks are more ubiquitous. Dragline silk is the best example of the jack-of-all-trades; most spiders use it for locomotion, and as a safety line. It also plays a role in chemical communication, allowing male spiders to determine the sex and direction of the owner of a dragline (Tietjen and Rovner, 1980). In addition, web-building spider will make web- supports or entire webs out of dragline.

When spiders move, they invariably leave a train of dragline behind which is attached to the substrate in intervals. If the spider where to fall, the dragline can prevent the spider from hitting the ground and doing itself damage. Furthermore, escape behaviours using dragline are common – spiders will fall away from the disturbance, using their dragline to bring them to a stop. This also allows them to climb back up to their former location, a distinct advantage if their have a web to return to.

Dragline is used for locomotion in two ways. Firstly, it allows spiders to drop down from and climb back up to a previously accessed location. Secondly, by spooling out lengths of silk and letting air current pick them up, spiders can essentially fly. Ballooning, as this behaviour is called, is a common dispersal mechanism – the first animals found on Krakatoa a year after it exploded in 1883 were web-building spiders that had been carried there by the wind (Bristowe, 1931). Air drag is also used by spiders, like the orb weaver *Araneus diadematus* Clerck 1757 to build webs that span a gap, sometimes of several meters or more. Walking from one support to the other is not an option; instead the spider spools out silk and lets wind currents carry the silk across the gap. Once the silk gets tangled up on the other side, the spider anchors a dragline and pulls itself across the space. This lets the spider construct a web where it normally couldn't reach. In addition, the structural support of all webs is built entirely out of dragline. Web strength, energy dissipation and signal transmission are part of the function.

The orb weaver *A. diadematus* and the jumping spider *Salticus scenicus* Clerck 1757 are examples of spiders with very different lifestyles that are reflected in how dragline is used. The orb weaver like *A. diadematus* build circular webs

with dragline frames, and capture spiral from viscid silk. The supporting lines area made up of one or more strands of dragline, but long support lines or webs in windy locations are often reinforced with 14 strands or more (personal observation). The radii that connect the central hub to the supports is made of single strands of dragline and act as a framework for the viscid silk spiral which covers most of the circular area of the web. The spiders will sit in the hub, or in a retreat with a signal line connected to the hub with which they can sense vibrations caused by prey impacts. The radii also act to transmit vibrations to the spider. Therefore, dragline pays an important role in giving the web its shape, strength and ability to transmit vibrations.

Jumping spider are active hunters that stalk their prey and only a few species build primitive webs for catching prey (Hallas and Jackson, 1986). These spiders have excellent eye sight, with colour vision and good resolution, and make good use of this to track their prey (Williams and McIntyre, 1980; Jackson and Wilcox, 1998; Robinson and Valero, 1977). Dragline is very important in that it allows vertical locomotion, and acts as a safety line in the event of a fall or unsuccessful jump.

The question this thesis will attempt to answer is how well suited dragline silk is as a safety line. Chapters 2 and 3 were written as independent studies to be submitted for publication. Chapter 2 focuses on how the safety factor scales relative to body mass, and concludes that dragline from adult *A. diadematus* and all *S. scenicus* is too weak to absorb the energy of a fall in which no additional silk it produced by the spiders. Chapter 3 characterizes the properties of three fiction brakes available to the spider, and finds that under normal conditions *A. diadematus* has a dynamic safety factor between 6 and 2, while *S. scenicus* has a dynamic safety factor of 1.

Space filler #1 ~ A cluster of first instar *Araneus diadematus* after leaving the cocoon. The spiders will disperse after a few days and start building webs.

Chapter 2: The Scaling of Safety Factor in Spider Dragline

Introduction

The relationship between a material's properties of a structure and its function are a common theme in engineering. The safe construction of bridges, buildings and vehicles for example, depends on understanding how a material responds to both normal and peak forces imposed during the intended lifespan of the structure. Making strong structures, however, cannot be the only objective, since cost has to be considered as well. Hence balancing these different constraints is an important part of design. A common measurement of the quality of design in a structure limited by tensile strength is the safety factor, or the ratio between material strength and maximum load. In an efficient design the safety factor approaches 1.0 because the strength is exactly matched to the load. Because of variability in material properties and uncertainties in the loading regime, safety factors must exceed this theoretical optimum for the structure not to fail in normal use (Alexander, 1996). For example, under British Standards bs 449, a steel member under tension, with a yield stress of 2.5×10^8 Pa, may not be loaded to more than 1.65×10^8Pa, an effective safety factor of 1.5 (Blockey, 1980).

Biological structures are similar in that design is shaped by a number of constraints. Even if the cost of failure is high, greater strength is offset by higher structural cost. The assumption that evolution would eventually lead to a decent compromise is not unreasonable. An optimal solution is, however, unlikely ever to be achieved in any biological system simply because parameters change with time. In fact, a "sufficient" solution can be good enough unless additional selective forces act on the system.

An example of this are pigeon feathers. As weight at the end of a flapping wing increases the cost of locomotion considerably, feathers would be expected to have low safety factors – the cost of use would be greater than the cost of failure (Alexander, 1981 referenced in Corning and Biewener, 1998). What Corning and Biewener (1998) showed, however, is that the safety factor of the flight feather shafts is 6 to 12 during strenuous flight, which is much less than the estimated safety factor of 2.2 for the humerus bone (Kirkpatrick, 1994). The explanation proposed is that, unlike wing bones, flexural stiffness is the driving factor in feather evolution rather than strength.

Spider silk also is interesting in this respect because it is a structural material that has been made by spiders for at least 380 million years (Sheldon et al., 1991) and has evolved into eight different types with different uses and properties. Dragline silk, in particular, is made by the vast majority of spiders, from first instars to adults, and is used for a wide variety of purposes including locomotion, safety lines, web construction, signal threads and chemical communication (Foelix, 1996; Tietjen and Rovner, 1982). Spiders that make dragline, no matter what its other uses, will trail out this silk behind them as they walk around, attaching it to the substrate at intervals. The dragline can then act as a safety line in the event of a fall (Brandwood, 1985).

When the spider descends or falls, a successful safety line stops the falling spider without breaking the safety line, and the spider can either climb back up or descend further. Safety

factor can be used to evaluate the efficiency of dragline as a safety line, and one method is to calculate the static safety factor ($F_{MAX,\ BW}$), which can be calculated as the breaking force (F_{MAX}), divided by spider's weight Mg,

$$\text{Static safety factor} = F_{MAX,BW} = \frac{F_{MAX}}{Mg} \qquad (2.1)$$

The subscripts max and bw are used to indicate breaking forces and forces expressed in spider body weights respectively.

Osaki (1996) calculated that adult *Nephila clavata* dragline has a static safety factor of 6, which is higher than what would be expected for an efficient design. The static safety factor, however, does not take into account the true function of the safety line, which is rarely used as a static support. It virtually always functions dynamically when loaded in impact, where it must absorb the energy from a falling animal, and therefore body weight underestimates the true functional load.

The scenario I chose to investigate is a spider with a length of attached silk that falls without reaching terminal velocity, and no additional silk is produced. If the safety line's attachment is at the same height as the spider, the spider is initially in free-fall until the length of silk runs out, and the dragline is loaded in impact. This scenario is essentially a bungee jump (see Figure 2.1a).

A safety line absorbs the energy of a falling spider by being stretched, and the greater the stretch the lower the impact force. This relationship arises from Newton's Second Law,

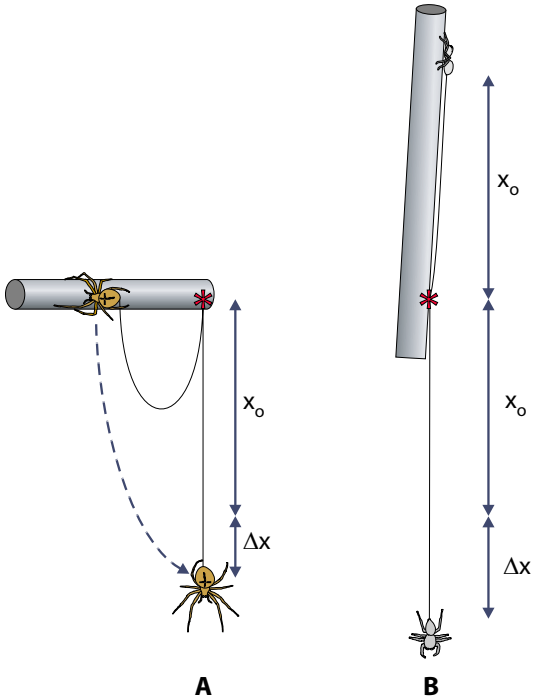

Figure 2.1 Overview of bungee jumping spiders. On the left is a spider bungee jumping with pre-made silk of length x_o. The silk attachment point is marked with a red star. When the silk starts to take the load of the spider, x_o below the attachment site, the silk is stretched Δx before the spider comes to a stop. On the right is a worst case scenario in which the spider falls $2x_o$ before silk is loaded.

$F=Ma$, because greater stretch implies lower deceleration and hence lower impact force. Thus, the actual dynamic safety factor is determined by the stretchiness of the material as well as the strength of the fibre. In the analysis below I model the dynamic loading of the safety line in terms of

breaking force of the fibre F_{MAX} and the breaking strain ε_{MAX} of the spider's silk.

We assume that the dragline functions as a linear spring, and so spring stiffness (k) is expressed as

$$\text{Static safety factor} = F_{MAX,BW} = \frac{F_{MAX}}{Mg} \tag{2.2}$$

Thus, dragline stiffness is derived from the ratio of breaking force (F_{MAX}) and the breaking strain (ε_{MAX}). Since strain, $\varepsilon = \Delta x / x_o$ where x_o is the unstretched length of the fibre and Δx is the distance the silk stretches to stop the spider (see Figure 2.1a), then

$$k = \frac{F_{MAX}}{\frac{\Delta x_{MAX}}{x_o}} \tag{2.3}$$

The energy absorbed in the extension of the silk fibre (E_S) is

$$E_S = \tfrac{1}{2} F \Delta x \tag{2.4}$$

and by substituting equation 2.3 we obtain the maximum energy absorbed by stretching a silk fibre to it's failing point,

$$E_S = \frac{k}{2x_o}(\Delta x_{MAX})^2 \tag{2.5}$$

Failure of the fibre will occur when the energy released in the fall exceeds the capacity of the silk to absorb energy. During the free-fall, the gravitational energy released is Mgx_o, and as the fibre stretches the additional gravitational energy is $Mg\Delta x$. Thus, the energy release at fibre failure is

$$E_G = Mgx_o + Mg\Delta x_{MAX} \tag{2.6}$$

When E_S is equal to E_G, the safety line can just support the impact load, so the dynamic safety factor is equal to 1. At this condition

$$Mgx_o + Mg\Delta x_{MAX} = \frac{k}{2x_o}(\Delta x_{MAX})^2 \tag{2.7}$$

and by rearranging and substituting equation 2.1 and 2.2, we calculate the static safety factor ($F_{MAX,BW}$) required for a material with a given extension to failure (ε_{MAX}) as

$$F_{MAX,BW} = \frac{2}{\varepsilon_{MAX}} + 2 \tag{2.8}$$

If the spider climbs above the silk's attachment point, however, more gravitational energy has to absorbed by the silk, and this represents the worst case scenario. In this case, the spider falls from a distance x_o above the attachment point (see Figure 2.1b), such that the total distance of the fall is $2x_o + \Delta x$,

$$F_{MAX,BW} = \frac{4}{\varepsilon_{MAX}} + 2 \tag{2.9}$$

predicts the static safety factor required.

Two examples illustrate how breaking strain and static safety factor interact. Kevlar is a man-made material with exceptional stiffness and strength, but low breaking strain. The breaking strains for single filaments of two types, Kevlar 29 and Kevlar 49, are in the range of 0.028 to 0.036, and the

minimum static safety factor required for a Kevlar safety line would be 58 to 75 according to equation 2.8 (see Figure 2.2). Also shown is natural rubber, which is at the opposite end of the spectrum with low strength and stiffness, but very high breaking strains. With maximum strains of 2.5 to 6, static safety factors would need to be in the order of 2.3 to 2.8 for a successful bungee jump. This comparison clearly shows that the safety line made with stretchier material will not need to be as strong to successfully absorb the impact of a bungee jump. Furthermore the range of static safety factors associated with a range of strains becomes smaller as the material becomes more extensible because equation 2.8 is an inverse function with a slope that changes from vertical to horizontal with increasing strain. Because there is variation in the property of any material, the range of minimum static safety factors needed for a bungee jump decreases as the material increases becomes stretchier and as a consequence, one would expect lower safety factors.

The properties of dragline silk are well known for a number of species (Stauffer et al., 1994; Gosline et al., 1986; Köhler and Vollrath, 1995), and these studies include values for breaking strain, which fall in the range of 0.2 to 0.35. This suggests that minimum static safety factors would to be between 7.7 and 12. Thus the static safety factor of 6 observed by Osaki (1996) for adult *Nephila clavata* dragline suggests that dragline cannot function as safety lines in bungee-jump falls. This is surprising if one considers that 380 million years should be enough to match property and function for something as important as a safety line. Brandwood (1985) showed that the silk from the argiopid spider *Meta segmentata* would break during a worst case scenario where the animal falls

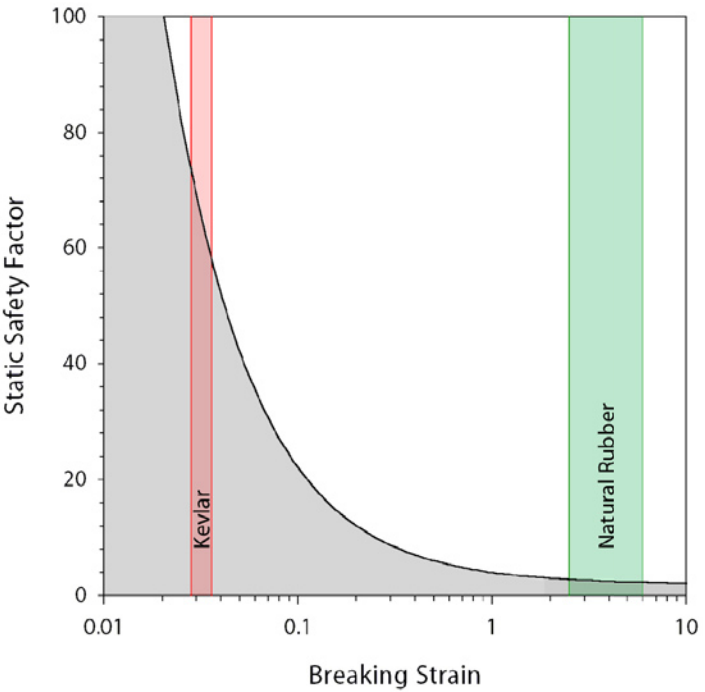

Figure 2.2 The effect of breaking strain on the minimum static safety factor needed for bungee jumping. When a dynamic safety factor of 1.0 for bungee jumping (—) is combined with the strain of failure of several common materials, we can determine how much stronger a single filament rope would have to be than the mass of its load to support it during a bungee jump. The shaded area represents strain - safety factor combinations that would fail during bungee jumping. For example, for a strand of Kevlar would have to have a static safety factor of at least 75, while natural rubber would only need a safety factor of 2.8 or more. The strain values were obtained from Glen Martin Engineering, Inc. (www.glenmartin.com/industrial/pg37.htm) and RFI Seals & Gaskets Ltd (www.rfiseals.co.uk/documents/solidrubbelastomeric.htm).

from above its attachment point, but it remains to be seen if dragline is suitable for bungee jumping.

In this study I present data on the scaling of mechanical design in spider safety lines in two species, the orb weaver *Araneus diadematus* and the jumping spider *Salticus scenicus*. I show that the mechanical properties of dragline silk, such as tensile strength and extensibility, remain unchanged over the full range of size in *A. diadematus*, from 0.0004 g first instar hatchlings to 1.2 g gravid females. In contrast, the silk cross-sectional area and breaking force scale strongly with body mass. The pattern of scaling produces static safety factors that decrease with increasing spider mass, such that only the smallest individuals can safely bungee jump. Preliminary data for *S. scenicus* indicate a similar relationship, but static safety factors are below the threshold over the entire size range.

Materials & Methods

Spiders

Dragline was gathered and tested for *Araneus diadematus*, an orb weaver, and *Salticus scenicus*, a small jumping spider. Adult spiders were collected from July to November locally in Vancouver, B.C., and kept indoors with a 14/10 hour day/night cycle at ambient temperatures. The orb weavers were placed in 60 cm × 60 cm × 10 cm wooden boxes with Plexiglas sides, while the jumping spiders were kept in 500 ml glass jars with a large twist of paper for increased surface area. Spiders were misted every few days and fed with a variety of insects once or twice per week.

To obtain silk from the entire weight range of *A. diadematus*, an egg case was hatched in the laboratory, and dragline was taken from the spiders as they grew. Silk was obtained by taking the spider on a hand, waiting for it to attach the dragline to the hand and then gently brushing it off so that it dropped on its dragline. This dragline was wound up on a small cardboard frame while the spider hung on the silk. Immediately afterwards, the spider's weight was measured on a Mettler H31 (±0.1 mg) or Mettler H54 (±0.01 mg) microbalance.

Samples of jumping spider dragline could not be obtained in the same way, as they jumped off of the hand without an attached dragline more often than not. These spiders do, however, spool out dragline as they move around, so the silk was collected by putting a spider in a plastic container and picking up the silk behind it. Because one adult female laid eggs, two samples of silk were obtained from very young *S. scenicus* in addition to adult silk. Unfortunately these juveniles could not be raised in the laboratory so silk could not be tested from medium sized *S. scenicus*.

For adult spiders, silk diameters were measured using a Wild m20 microscope under polarizing light with a 100× oil immersion lens and 15× Wild filar micrometer. A width of a double stranded piece of silk was measured and the distance divided by 2 to get the diameter for a single strand of silk. Silk from smaller spiders and selected adults was sputter coated with gold and placed in a Cambridge 250t scanning electron microscope for measurement. Photos were taken at magnifications ranging from 18,000× to 100,000×, and silk diameters were measured and converted using the

scale bars. With one exception, all silk sampled was double stranded, as is the norm. One adult *A. diadematus* spider, however, produced dragline with three strands of equal diameter.

At least one piece of silk was tested for each spider. When multiple samples from a single piece of silk were tested, the results were averaged to avoid pseudo-replication. All silk was tested to failure starting from slightly slack silk, and tests in which silk broke within 2 mm of either attachment point were damaged by the gluing process and discarded. The silk length at which the first rise in force was observed was taken to be the initial length (x_o) and used to calculate instantaneous strain. To compensate for the 4000 fold range of spider weights, force was expressed in spider body weights by dividing the breaking force (N) of a spider's silk by that spider's weight, Mg (N) because the body weight is the relevant functional unit for a safety line. Additionally, breaking force (N) was converted to breaking stress (Pa) by dividing by the total cross-sectional area (m^2) of silk when known. The initial slope, or initial modulus (Pa), was calculated from the resulting stress-strain data by fitting a least-squares regression to the linear portion of stress-strain curve before the yield point. The yield strain was determined to be the point at which the dragline's stiffness decreased after an initial stiff region.

Quasi-static testing

Because of the large range of spider weights and corresponding silk breaking forces, two different methods were used to measure the failure force of the silk. Most spiders weighing more than 0.150 g were tested on an Instron model 1122 tensile testing machine with a custom built stain gauge force transducer with a 100 g full scale sensitivity.

Table 2.1 Summary of average dragline material properties ± SE, (n). Two tailed t-tests were used to identify significant differences between the two species ($P^* = 0.0075$, $P^{**} = 0.014$, $P^{\#} = 0.027$)

	A. diadematus	*S. scenicus*
Yield Strain	$0.034 \pm 0.003^*$ (14)	$0.056 \pm 0.001^*$ (2)
Breaking Strain	0.251 ± 0.009 (35)	0.248 ± 0.040 (4)
Breaking Stress (GPa)	1.31 ± 0.08 (12)	1.66 ± 0.28 (2)
Initial Modulus (GPa)	$12.3 \pm 1.0^{**}$ (12)	$19.7 \pm 0.2^{**}$ (2)
Scaling exponent	$0.743 \pm 0.028^{\#}$ (33)	$0.539 \pm 0.0842^{\#}$ (4)

Silk samples were glued with Loctite Superbonder 409 cyanoacrylate superglue, 5 Minute Epoxy or nail polish onto thin cardboard from which a 6 cm windows had been cut,. This frame was mounted in the Instron and the cardboard carefully cut away to expose the silk. If necessary, crosshead distances were adjusted to make the silk slack. Crosshead speed was set to 3.3×10^{-4} m s^{-1}, giving strain rates of 0.0056 to 0.0066 s^{-1}.

Silk from smaller spiders proved to be too weak to be measured accurately with the Instron, so an alternate set-up using glass rods was used as described in Pollock (1991). Briefly, a glass rod of known stiffness (E) and radius at tip (r_T)

and base (r_B) is glued parallel to a glass slide. If silk is glued to the glass rod at distance l from the base, any deflection (d) of the rod at the attachment point can be used to calculate the force acting on the rod:

$$F = \frac{3\pi E r_T r_B^3 d}{4l^3} \qquad (2.10)$$

One end of a 3.4 - 5.7 cm piece of silk was glued with Loctite Superbonder 409 cyanoacrylate or 5 Minute Epoxy to the glass rod, and the other end to a hook pulled by a variable speed dc motor set to 2.27×10^{-4} m s^{-1}, giving a strain rate of 0.0057 to 0.0093 s^{-1}.

To measure rod deflection, the glass rod was placed under a Wild m21 microscope with a 4× or 10× objective lens and projected onto a TV. Deflection was measured with a video dimensional analyser (Instrument for Physiology & Medicine, model 303) by measuring the movement of the rod boundary at the attachment point relative to an arbitrary reference point. Voltage output proportional to rod deflection was collected by chart recorder and/or PC computer with LabTech Notebook 6.1.2 or LabView 5.0, and a calibration slide was used to determine a voltage per distance calibration.

Results

Silk was collected from the entire size range of *A. diadematus* spiders, from 0.00036 g first instar hatchlings to gravid 1.15 g females, with silk tested from 35 individuals. Silk samples from *S. scenicus* were sampled from two adult and two first instar spiders. Figure 2.3 shows sample silk tests

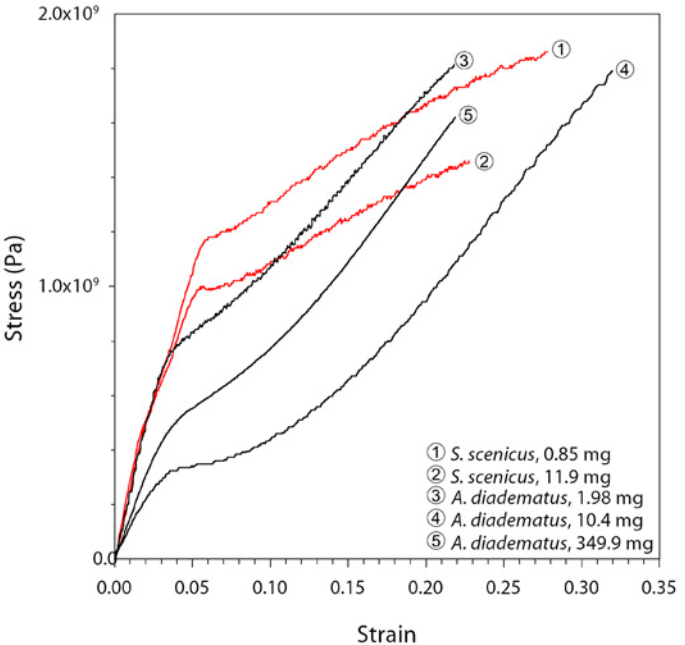

Figure 2.3 Sample data from several silk tests to failure from juvenile and adult spiders. *Salticus scenicus* are shown in red, and *Araneus diadematus* in black. Note the difference in shape between the two species.

to failure from juvenile and adult spiders of both species. The tests were chosen to show the full range of stress-strain curves possible. All samples showed a initial region of high stiffness followed by a yield point, where subsequent stiffness is dramatically reduced. In *S. scenicus*, the lower stiffness was maintained to the failure point, giving a "two-slope" curve. On the other hand, in *A. diadematus* silk the stiffness frequently rose again before failure, resulting in a "three-slope" curve. Table 2.1 summarizes the data that have

been derived from these tests, namely breaking strain, yield strain, breaking stress and initial modulus.

Analysis of the mass dependence of material properties revealed that there were no significant effects of body mass on breaking strain or on the initial modulus. Figure 2.4 displays data for the scaling of breaking strain observed for 35 samples from 24 *A. diadematus* individuals and the least squares regression slope is not statistically different from zero (P = 0.14). Four samples from *S. scenicus* show similar values, but the small sample size makes it impossible to separate species and size dependent differences.

Figure 2.5 shows that there was no effect of body mass on silk strength. The easiest method to determine if breaking stress in constant over a range of weights is to graph stress against mass. If the slope of the regression is different from zero, breaking stress is not constant and changes as the spiders grows heavier. The statistically stronger method is to determine if the slope of breaking force plotted against cross-sectional area is linear because the slope, or force per cross-sectional area, is equivalent to breaking stress. Therefore when both axes are log transformed, the slope of the regression will indicate whether the relationship of non-log transformed data is constant or variable because the slope is equal to the exponent of a power function. If the slope is 1.0, then the relationship is linear, while any other value indicates in a non-linear power function with changing slope. As Figure 2.5 shows, not only is the regression a good fit through the combined data from both species, the slope of 0.95 ± 0.03 (sd) is not statistically different from 1.0 (two tailed t-test, $P = 0.14$). Average stress at failure is therefore

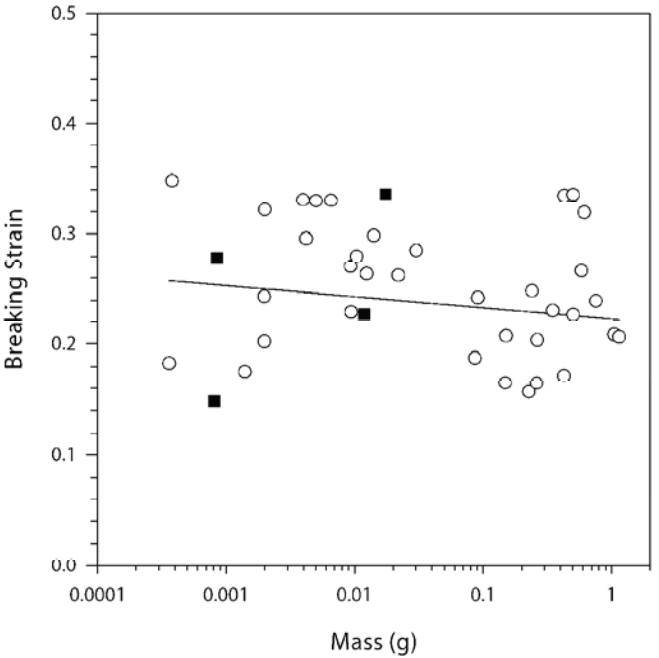

Figure 2.4 The breaking strain is normally distributed ($P = 0.54$) with an average of 0.25±0.009 (SE), for combined data from both species; *A. diadematus* (○), *S. scenicus* (■). There is no statistically significant trend with log transformed spider mass (M). The least squares regression best fit was $\varepsilon_{max} = 0.235 - 0.01 \log M$, $r^2 = 0.03$, $P = 0.27$.

independent of body weight and species, and thus the breaking force of the dragline depends only on its cross-sectional area.

While both species have the same average breaking stress, the relationship between cross-sectional area and spider mass is quite different (Figure 2.6) with *S. scenicus* having much thinner silk than *A. diadematus* for spiders of the same

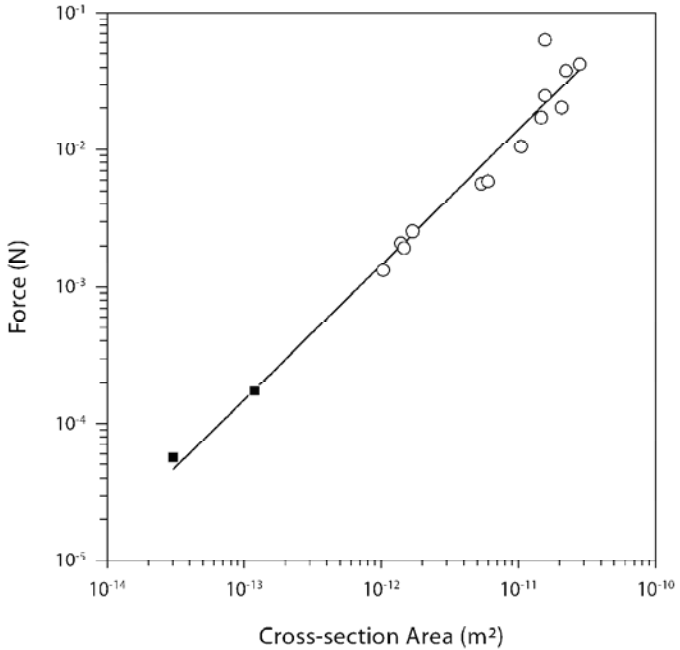

Figure 2.5 Breaking force graphed against the silk's cross-sectional area. The combined *A. diadematus* (○) and *S. scenicus* (■) force scaled as $9.90\times10^{8}A^{0.986}$, r^2=0.97, $P < 0.000001$, where A is cross-sectional area.

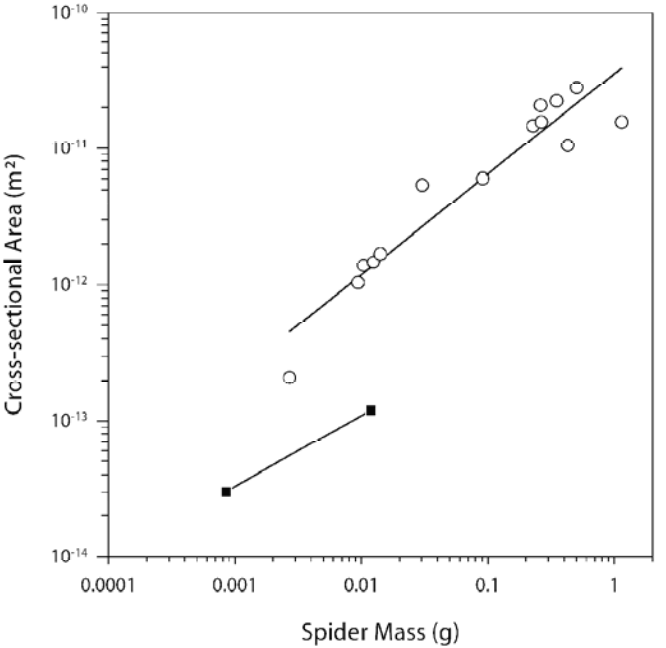

Figure 2.6 Cross-sectional area plotted against spider mass with a least squares regression applied to log-log transformed data from *A. diadematus* (○) and *S. scenicus* data (■). Area scales as $3.55\times10^{-11}M^{0.739}$, r^2=0.90 for *A. diadematus*, and $1.17\times10^{-12}M^{0.517}$, r^2=0.90 for *S. scenicus*, where M is spider mass.

weight. From this we would predict that there are going to be large differences in safety factor between the two species. This is confirmed in the scaling of the dragline breaking force.

As Figure 2.7 shows, the breaking force of dragline silk scales with body mass as

$$F_{MAX} = 0.049M^{0.74} \qquad (2.11)$$

for *A. diadematus* and

$$F_{MAX} = 0.002M^{0.54} \qquad (2.12)$$

for *S. scenicus*, which are statistically different (two tailed t-test, $P = 0.027$). Three silk samples had been tested from first instar *A. diadematus*, but because the breaking force for these spiders fell well below the best fit for the other spiders, they were excluded from the calculation as outliers.

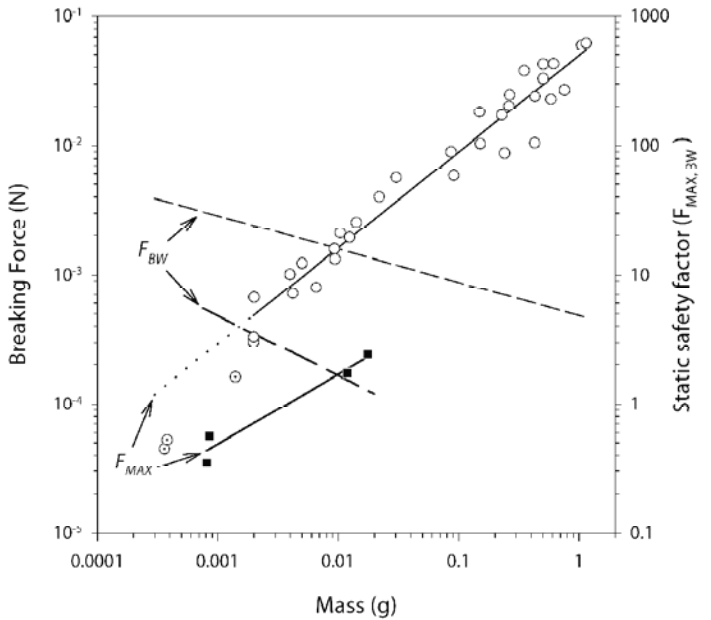

Figure 2.7 Breaking force scales as $0.049M^{0.743}$, $r^2 = 0.96$ where M is spider mass for *A. diadematus* (⊙), and as $0.002M^{0.539}$, $r^2 = 0.96$ for S. scenicus (■). The first instar *A. diadematus* (⊙) were excluded as outliers and fall well below the extended best fit line (dotted line). The force-mass scaling relationship for *A. diadematus* is also graphed as force in spider body weights (—) on the secondary y-axis as $F_{MAX, BW} = 5.03M^{-0.257}$ for *A. diadematus* (– – –), and $F_{MAX, BW} = 0.206M^{-0.461}$ for *S. scenicus* (– – –), where $F_{MAX, BW}$ is the static safety factor and M is spider mass.

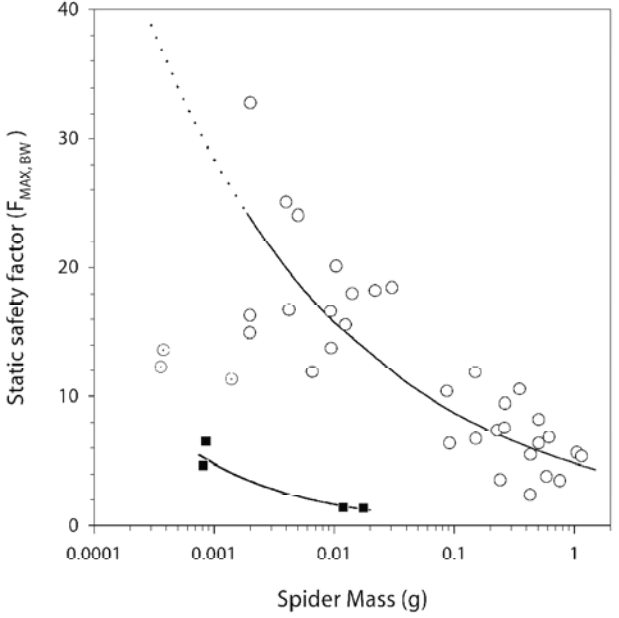

Figure 2.8 Static safety factor graphed against spider mass for first instar *Araneus diadematus* (⊙), *A. diadematus* (⊙), and *S. scenicus* (■). The best fit power functions from figure 2.8 are expressed in static safety factors and included. For *A. diadematus* (–) $F_{MAX, BW} = 5.03M^{-0.257}$and for *S. scenicus* (——), $F_{MAX, BW} = 0.206M^{-0.461}$, where $F_{MAX, BW}$ is the static safety factor and M is spider mass. Note that the first instar spiders are well below predicted values.

The consequence of this scaling relationship is that when breaking force is expressed in body weights rather than in Newtons, the relationship becomes

$$F_{MAX, BW} = 4.84M^{-0.26} \qquad (2.13)$$

for *A.diadematus* and so the safety factor is expected to decline with spider mass.

The same data, with force expressed in body weights (i.e. static safety factor), is shown in Figure 2.8 and clearly demonstrates that the relationship between spider mass and

strength is not constant or even linear. The best fit power function from Figure 2.7 was added to the data and supports the observation that adult *A. diadematus* spiders have silk capable of supporting 4 to 6 body weights, while the static safety factor for juvenile silk can be as high as 30. Again, first instar silk breaking forces were well below the predicted values.

Force and strain at failure are an indication of how much energy dragline can absorb before breaking, and when force is expressed in body weights, it takes the load into account during a fall. Figure 2.9 combines these data with equation 2.8 to graphically show that the silk from all *S. scenicus* and all adult *A. diadematus* weighing more than 0.1 g would fail in a bungee jump. Lighter spiders with higher static safety factors fare much better, some even capable of supporting of two or three times their weight. Clearly spider draglines fail to meet the requirements for bungee jumping.

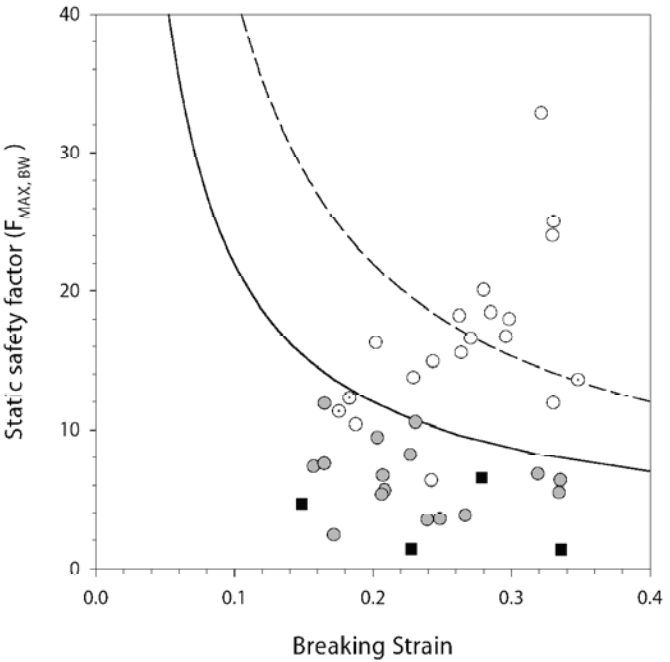

Figure 2.9 Graph of static safety factor against breaking strain as in figure 1 but scaled for silk data. Curves for dynamic safety factors of 1 for bungee jumping (——) and a worst case (- - -) were included to predict whether silk of know force and strain at failure would support a spider successfully under these conditions. Silk with properties that place below the dynamic safety factor would not survive a bungee jump while only silk above both lines would be suitable for a worst case scenario. As in other graphs *S. scenicus* (■) are shown while *A. diadematus* are roughly separated into first instar (⊙), < 0.1 g juveniles (○), and > 0.1 g adults (◉).

Discussion

It is surprising that *A. diadematus* and *S. scenicus* dragline should have the same average breaking stress and strain properties given the number of differences not only in how dragline is used, but also in other material properties. Firstly, *S. scenicus* stress-strain curves have two slopes while *A. diadematus* dragline tensile tests result in a wide variety of shapes, from simple double slopes to complex curves with three or more slopes (see also Pollak 1991). And secondly, dragline from the jumping spider *Metacyba undata* contracts to 95% when placed in water (Work, 1981), and it is likely that *S. scenicus* dragline reacts in a similar manner.

Araneus diadematus dragline will supercontract to 55% under the same conditions (Work, 1981). Whether the similarity in breaking strain and stress is anything more than coincidence is debatable, but it does mean that *S. scenicus* have lower static safety factors only because the silk is thinner, not because it is inherently weaker.

The fact that the scaling exponent for the breaking force – spider mass relationship came out as 0.74 for *A. diadematus* cannot be explained by geometric growth of the exoskeleton, which would result in an exponent of 2/3. Body dimensions, such as leg length, scale geometrically with weight increase (Prange 1977) and therefore the silk spinning structures, i.e. the spinnerets, will most likely also scale geometrically. Silk diameter can, however, change during an instar (Witt et al., 1968; Vollrath and Köhler, 1996) and is therefore independent of exoskeletal size. Hence if silk diameters were scaled to maintain a constant static safety factor, the exponent should be 1. This is what would be expected if dragline were optimized to minimize cost, and since the average breaking strain is 0.25, a static safety factor of 10 would fulfill the minimum requirements for bungee jumping. The consequence of the observed non-linear force-mass relationship is that juvenile spiders have proportionally stronger silk that adult spiders, and therefore dragline with higher safety factors.

The scaling exponent of 0.54 for *S. scenicus* cannot be easily explained either. Again, it matches neither geometric scaling nor minimum cost, and does not follow the same relationship as *A. diadematus*. But with only 2 data points at each end of the spider's range, the accuracy of the scaling exponent is suspect and more data is needed before any comparisons can be made.

From Figure 2.9 we know that dragline silk is too weak for bungee jumping for *A. diadematus* weighing more than 0.1 g, and only a few < 0.1 g spiders have silk that would not break during a worst case jump from x_o above the silk attachment point. This is surprising considering that a fall onto a flat surface from as little as 1 meter can be a terminal experience for large gravid *A. diadematus* females (personal observation). One would expect that especially these spiders would have safety line sufficiently sized to stop a fall, since eggs can not be laid if the spider dies prematurely. Additionally, small spiders are not harmed by falling, and the very smallest spiders have been observed floating away in the smallest breeze before they hit the ground and so would hardly need such a strong safety line. In fact, Fabre found that a beam of sunlight onto a carpet in a closed room caused an updraft that was enough for freshly hatched spiders to balloon to the ceiling (Crompton, 1951).

One possible explanation for the exceptional strength of draglines from small *A. diadematus* spiders is that wind loading acting on orb webs is likely to be similar for large and small webs. This is because the dragline's small cross-sectional area has a flow state indicated by the low Reynolds number of approximately 0.2. Drag (D) on a piece of silk with radius (r), length (l), in a wind velocity (v) and dynamic viscosity (μ) can be calculated by the following equation for cylinders with very small Reynolds numbers (Vogel 1994)

$$D = \frac{4\pi l v \mu}{ln(1/r) + 0.193} \qquad (2.14)$$

Given that μ is 1.8×10^{-5} kg m^{-1} s^{-1} and assuming a wind velocity of 10 m s^{-1} acting on a 1 m length of silk from a small second instar spider (r = 250 nm) with silk perpendicular to the flow,

the drag acting on the thread is 1.5×10^{-4} N, irrespective of the dragline doublet's orientation to the wind. This is close to the estimated breaking force of 6×10^{-4} N for spiders that size. The largest diameter measured from an adult spider, 3.7 μm, will only experience a 15% greater force from the same wind. Therefore the minimum strength of the silk for juvenile spiders is likely not determined by body weight or the size of the intended prey, but by the action of the wind on dragline in the web; dragline is scaled for web construction, not as a safety line. For larger spiders, the forces generated by the body weight or by larger prey would exceed the effect of wind, and therefore have more effect on defining dragline strength. Furthermore, making silk with larger cross-section costs more protein, and so gravid females may be sacrificing silk strength in favour of egg production.

That the first instar *A. diadematus* spiderlings fell below the calculated trend is not surprising. After the spiders emerge from their cocoon, they spend several days sitting in a clump before dispersing to build individual webs (personal observation). Until they catch something, they will not have eaten. In fact, even once they build their webs, prey items small enough to catch safely are few and far between, and the spiders mostly survive on the pollen carried onto the sticky viscid silk by the wind (Smith and Mommsen, 1984). Therefore it is not surprising that these very food limited spiders would produce thinner silk as a method of saving energy until prey becomes easier to catch.

While *S. scenicus* does not build webs, dragline does play an important role in prey capture. When catching large prey, a jumping spider may attack the prey and then jump to dangle by its dragline in midair while holding onto the prey (Robinson and Valerio, 1977). This has the advantage of making it difficult for struggling prey to get a foothold and wrench loose. It is also a useful mechanism to avoid aggressive ants summoned by the attack on a member of the colony (Robinson and Valerio, 1977). The fact that *S. scenicus* cannot bungee jump is not surprising since even adults are small enough to bounce without damage, and if they fall they tend to descend slowly like a rappelling climber rather than a bungee jumper.

It is very likely that first instar *S. scenicus* are as food limited as their orb weaving relatives, and that in order to survive, they must hunt prey as heavy or heavier than themselves. Having a dragline that can support the spider with large prey would be a distinct advantage. Adult spiders, on the other hand, have a greater range of prey sizes to choose from, and this may explain why the juvenile spiders have silk with higher static safety factors that the adults.

Clearly, draglines from *A. diadematus* and *S. scenicus* are not optimally designed for bungee jumping as defined by the standards of an engineer. That dragline is of great importance to both types of spider as safety line and a mode of transportation is clear (Robinson & Valerio, 1977; Gorb et al., 1998). Given that spiders have had 380 million years to fine-tune the relationship between material properties, structural design and function, the best explanation would be that the model is incorrect and/or our criteria for a good design are faulty.

The main assumption that goes into estimating silk energy

capacity is that silk stiffness is constant and that the energy capacity is therefore proportional to the area under the secant of breaking force. While this is a reasonable assumption for silk with pronounced three-slope curves as are common for *A. diadematus* (see Figure 2.3, ④), it underestimates energy capacity for two-slope curves like those of *S. scenicus* (see Figure 2.3, ① ②) by as much as 50%. As a consequence, estimates of dragline silk failing during bungee jumping are likely exaggerated.

Furthermore, silk from *A. diadematus* shows strain rate dependent properties, becoming stiffer, stronger and more extensible as it is stretched faster (Denny, 1976; Gosline et al., 1999). During a bungee jump, the safety line would be impact loaded at much greater speeds than the quasi-static conditions used for these experiments. Therefore, static safety factors would be higher when the silk is impact loaded by the spider's weight during a fall, but even with the two fold increase in breaking stress that occurs at strain rates of 20 – 50 s^{-1} (Gosline et al., 1999), adult *A. diadematus* safety line would still not be suitable for a spider falling from above its attachment point.

In addition, bungee jumping and the worst case scenario assume no additional silk is produced, but that is an artificial constraint since spiders can easily produce more silk on demand. A spider descending on a dragline while spooling silk is more like a rappelling climber than a bungee jumper, and because the silk is not impact loaded with the momentum of a freefalling object, the forces are significantly lower. Equations 2.8 and 2.9 would not apply, and the actual loading forces would depend on how quickly the spider decelerates, not the weight of the spider.

In summary, dragline silk is not designed for bungee jumping or worst case scenarios where no additional silk is produced. Behavioural adaptations such as silk spooling make a "perfect" design unnecessary. That dragline breaking force scales as a power function with spider mass likely has underlying reasons other than safety line design.

Chapter 3: Bungee Jumping with Friction Brakes

Introduction

A worst case scenario for a spider with a safety line would be a fall with a fixed length of silk. A bungee jump occurs when the silk attachment point and the start of the fall are at the same height and no additional silk is made. As spiders generally trail dragline behind them as they move, and attach it frequently to the substrate, bungee jumping as a scenario is not unreasonable. As a well designed safety line, the dragline has to be able to absorb the energy of the fall as well as the spider's weight when the spider falls.

Estimates of dragline's suitability as a safety line have been made by Osaka (1996) and Lucas (1964) for two different orb weaving spiders. Both concluded that the silk is more than strong enough to support the weight of the spider; however, Brandwood (1985) demonstrates that under dynamic impact loading the dragline fails. This is confirmed in chapter 2 where the adult orbweaver *A. diadematus* and the jumping spider *S. scenicus* are both found to make silk too weak to survive a bungee jump, much less a fall from above the attachment point – the worst case scenario.

Where the bungee jump scenario fails to model the way that spiders use their safety lines is that it is based on a fixed length of pre-existing silk. Spiders are very capable of producing more silk as they fall, and the production of more silk can dramatically alter the outcome of the fall. While the additional silk does not increase the silk's ability to absorb the energy of a fall, it does offer the possibility of using friction brakes to dissipate energy, much the way a rappelling human climber will run the climbing rope through a figure-of-eight descender to act as a friction gate. Any energy converted to heat by a friction brake would not have to be absorbed by the dragline, so is this the mechanism which prevents the safety line from failing?

As in the previous chapter, the static safety factor is inappropriate for evaluating dragline as a safety line when used for rappelling. This is because the applied force depends on how strongly and how many friction brakes the spider engages, not the material properties. For this reason, a "working" safety factor will be used in this chapter, and will be defined as the ratio of maximum force applied by a friction brake to the breaking force of the silk.

There are thought to be up to 3 friction brakes available to a spider. Firstly, the rearmost pair of legs can reach around and grab the silk. The tip of the tarsal segment has two or three claws which can pivot to trap silk against the numerous setae also originating from that area, thus forming a tension gate. The setae have serrated sides against which the silk is pushed, and when the claws pivot back, the silk jumps off the setae again (Foelix, 1996; Wilson, 1962b). By controlling how strongly the claws push the silk against the setae, different amounts of friction force could be generated. Since spiders can easily climb up their own safety line, it is likely that each leg is capable of applying at least one body weight of friction force, but as yet no attempts have been made to quantify this.

Since spiders can successfully accelerate and decelerate on

their draglines without the use of their legs (Wilson, 1962a), additional friction brakes must exist. Work (1978) suggested the spinnerets form a tension gate similar to that of the tarsal claws. The three pairs of spinnerets are under muscular control and can be pointed upward or pivoted laterally into a closed position along the midline. Work (1978) proposed that dragline leaving the spigots on the anterior spinneret would be forced to travel between varying amounts of silk spigots and setae de-pending on the proximity of the spinnerets to each other. With an open spinneret, dragline would exit free of spigots and setae, but as the spinnerets close, the increasing amount of interdigitation would force the dragline to travel a progressively torturous path. Movement of the spinnerets should therefore the correlated with changes in how much force it takes to pull silk out of a spider.

Finally, it has long been believed that an additional internal friction brake exists and is associated with the silk duct (Wilson, 1962a). Between the gland lumen and the spigot opening is a long duct with a number of associated structures. The orb-weavers in the families Araneidae and Tetragnathidae have a valve that is located close to the spigot exit which has been proposed to act much like a clamp (Vollrath and Knight, 1999), but this structure is absent except for a slight regional differentiation in other families (Wilson, 1962a). For a brake to exist, it must act on solid silk and be present in more than just the orb-weavers.

The orbweaver *A. diadematus* was chosen because it makes dragline that has well characterised properties, and its dragline uses are well known (Gosline et al., 1986, 1999; Wilson, 1962a,b; Work, 1977 & 1978). It is used for both web construction, locomotion and as a safety line. Furthermore, under most conditions, *A. diadematus* uses dragline freely for descents and it is co-operative when being forcibly silked. The jumping spider *S. scenicus* was chosen because it uses its dragline only for locomotion and as a safety line. This species is also particularly likely to jump and use its dragline for descents.

In this study I present data on the properties of the rear leg as a tension gate and the internal friction brake, and I propose a possible mechanism for the internal brake. The spinneret tension gate does not appear to function as proposed by Work, but both of the other two brakes are capable of applying at least two body weights of force. Video analysis was also used to estimate forces applied to a safely line when spider uses its dragline as a safety line under normal conditions.

Materials & Methods

Both species of spider were collected locally in Vancouver and on Salt Spring Island, BC, Canada. *A. diadematus* adult females were collected in the morning, silked and/or filmed and released the same day. Because *S. scenicus* are not as abundant, captured adults were kept in 500 ml glass jars in the laboratory and fed fruit flies once a week. Spider weights were measured with a Mettler H31 micro-balance (±0.1 mg) following each experiment.

Silk has to be drawn out of a spider; it is generally not extruded. Spiders attach dragline to substrate with glue

from the piriform glands and then draw out the silk by moving away or by descending and using their weight to pull the silk. Another method is to reach around with a rear legs to grab the silk and draw it out. It is common practice to take advantage of this drawing process to collect silk for experiments by forcibly silking them. Spiders are either encouraged to drop on their dragline, which is then reeled up and collected, or they are strapped down so that the dragline can be pulled out, often by attaching the silk to a motorized cylinder. In both cases the silk is under tension as it is pulled.

Friction Brakes

A set of experiments was designed to separate the different sources of friction (silk formation, internal or spinneret brake, and rear legs) and the contribution of voluntary and involuntary control. Spiders were filmed descending on draglines with a high speed video camera (MotionScope model 1108-002) connected to a PC computer. Sequences in which rear legs were not in contact with the dragline were analysed with Scion Image (beta 3b) to determine the angle at which the silk leaves the spinnerets. The angle varied, but its average was determined to be 160º from the ventral surface of the abdomen, or slightly ventral to straight out behind the spider.

The friction forces applied to dragline by a spider hanging from its dragline can be determined by measuring the force to draw silk from a spider attached to a force transducer. I used a semiconductor strain gauge force transducer connected through a preamplifier to a PC computer with LabView 5.0 for Windows. A small platform was screwed to the front of the transducer so that a spider could be tied firmly to the strain gauge with the spinnerets pointing up, and with the abdomen at 160º to horizontal (see Figure 3.1). Small masses of known weight were hung from the platform at various distances form the base of the transducer beam to establish a system calibration. This was necessary because spider dimension varied enough that the distance between spinneret and base of the transducer was not constant. A typical calibration was on the order of 30 V N^{-1}. Spiders were placed in CO_2 for 10 minutes to anaesthetise them and were then tied to the platform with the spinnerets exposed and accessible. Thirty minutes after removal from CO_2, dragline was pulled from the spider and taped to a motor mounted cylinder directly above the spider. Rear legs were prevented from grabbing the dragline unless otherwise stated.

The force transducer was prone to drifting in response to light and temperature fluctuations. Drift could be successfully corrected in for tests lasting less than one minute by assuming that the rate and direction of drift was constant. In those cases, a regression was fitted through the zero-force base line before and after silking, and used to correct the raw data. If drift exceeded 0.0005 V s^{-1} the test was discarded. Drift could not be corrected accurately when silking lasted for more than one minute because rate and direction of drift changed frequently.

The jumping spiders were not forcibly silked because of their small size (< 17 mg) and the very fragile silk resulted in silking forces too small for the force transducer used.

Owing to a five fold difference in *A. diadematus* mass, force was normalized by expressing it in terms of spider body weight (F_{BW}):

$$F_{BW} = \frac{F}{Mg} \tag{3.1}$$

where force (F) is in newtons, and Mg is the spider's weight.

Silking anaesthetised spiders

To determine how much of the friction brake is under neural control, spiders were silked while anaesthetised with CO_2. Spiders had been in CO_2 for at least 10 minutes before silking was started. Each spider was silked at 0.02 m s^{-1} and 0.002 m s^{-1} for 10 seconds. Forces were averaged for each period of silking.

Rear legs as friction brakes

To measure the rear leg's ability to apply friction force, spiders were tied to the force transducer with the left rear leg free. The dragline silk was pulled from the spider and attached to the motor directly above the spider. After the spider had been induced to grab the silk with its left leg, an extra 5 to 10 mm of silk were pulled out between the holding leg and the spinneret (see Figure 3.1). The motor was reversed until all the silk was slack, then set to one of two speeds, 0.02 m s^{-1} or 0.002 m s^{-1} and turned on. As the motor spooled up the silk, first the spider's leg holding the silk was raised, and then silk was pulled through the claws holding the silk. During the period before the silk between leg and spinnerets became taut, all the force resisting the

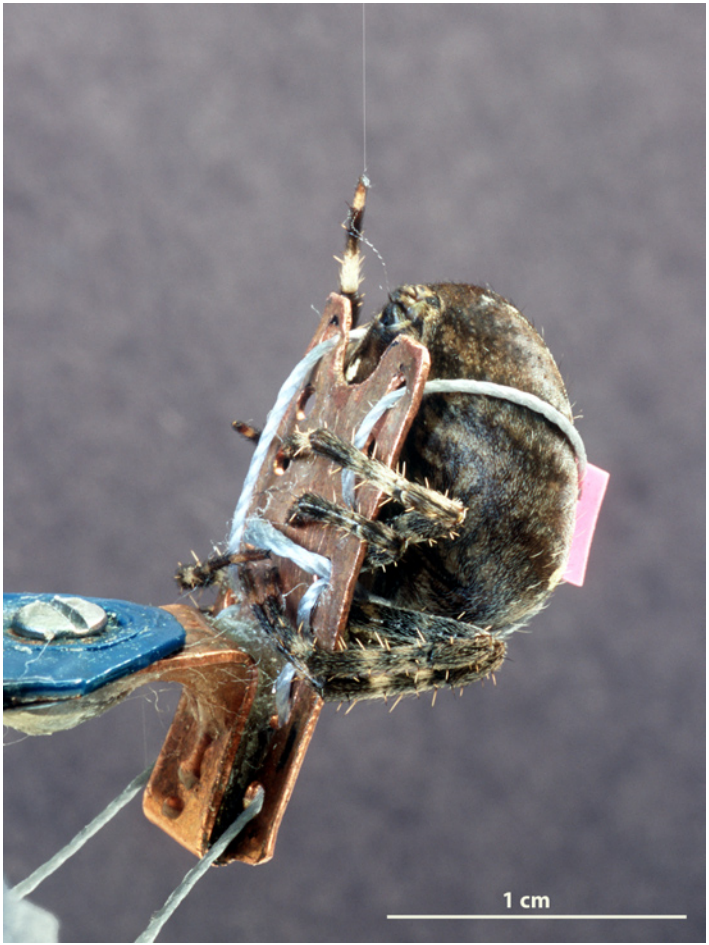

Figure 3.1 Close-up of spider tied to the force transducer while holding its dragline. Silk is taped to a spool directly overhead with the silk is drawn out at 160° to the ventral surface of the abdomen. Pieces of tape were used to as necessary to keep the rear legs from grabbing the silk. The spinnerets are in the closed position.

motor was the result of the rear leg only because no new silk was drawn. Average and peak values were calculated from force traces from the moment the leg started resisting until new silk was drawn from the spinnerets. Some spiders repeatedly released the silk with their leg, and the difference between the total forces before and after this event was considered the leg's contribution.

Internal friction brakes

Preliminary experiments suggested that the spider's internal friction brake might be silking velocity dependent. To test the hypothesis that friction force varied with silking speed, four silking speeds were chosen: 0.05 m s^{-1}, 0.10 m s^{-1}, 0.20 m $s^{-1}$and 0.30 m s^{-1}. The lower end of the range is well within the normal spider's behavioural range as determined from the video analysis of falling spiders. The upper range was the fastest speed that spiders could be consistently silked at. A single trial consisted of all four speeds (treatments) in pseudo-random order. For each speed the motor was turned on for 8 seconds, turned off, and then after a further 8 seconds the motor spool was slowly reversed until the silk was slack. The spider was given a further 16 seconds rest with the silk slack before the motor was turned on for the next speed. Each of the 13 spiders was only used for a single trial to minimize habituation or other learning effects. A black and white video camera was used to observe and record spinneret movements during silking in order to correlate spinneret movement with changes in force.

Silking to failure of silk

Preliminary data suggested prolonged silking could generate heat by friction which might contribute to silk failing, either by weakening the silk or by inducing the spider to cast off the dragline. This hypothesis was tested by selecting 15 spiders and silking each at one of three speeds (0.01 m s^{-1}, 0.10 m s^{-1}, 0.30 m s^{-1}) until the silk broke or ran out. Owing to transducer drift in response to ambient light and temperature fluctuations, the force data for tests lasting longer than 60 seconds cannot be considered accurate, but enough silk was obtained per spider to weigh on a Mettler H35 microbalance (±0.001 mg). Again, because of a five fold difference in spider weights, the silk mass was normalized by spider body weight.

Bungee jumping

To document the normal behaviour of spiders using dragline as a safety line, spiders were filmed with a high speed video camera (MotionScope model 1108-002) connected to a PC computer. The experimental arena was set up in a dark room, with a light source placed behind the camera, and a ruler suspended along one edge of the view field as a reference and calibration aid. A glass rod was mounted horizontally, perpendicular to the ruler (see Figure 3.10a) and spiders were placed on the beam and filmed at 250 frames/second as they moved around. By carefully selecting the right diameter of clean glass rod, an *A. diadematus* spider could be induced to move until it lost its grip and fell. Only sequences where the spider fell in the plane of focus were kept and analysed. *S. scenicus* were more difficult to work with - although they

jumped off the glass rod with little urging, they did not fall even when Teflon tape was placed on the rod. Because of this, only one film sequence shows a fall with any premade silk, as opposed to a jump which involves the immediate production of more silk.

Between 2 to 5 falls were recorded and analysed for each of the 3 *S. scenicus* and 8 *A. diadematus*. Digital film sequences were separated into individual bitmaps with AVI Constructor 3.0 and analysed using Scion Image (beta 3b). The approximate centre of mass and the attachment point of the silk to the rod (when visible) were selected for each frame of a series and given x-y co-ordinates. Two passes with a second order, zero phase shift Butterworth digital filter (Winter 1990) were used to mathematically smooth the x-y co-ordinates. Cut-off frequencies of 35 to 50 Hz were carefully selected to prevent oversmoothing. The smoothed positional data were used to calculate the instantaneous velocity between two frames. Pixels per centimetre were calculated for each fall from the ruler, and were used to covert pixel dimensions to SI units.

For spiders falling vertically, with little or no horizontal swinging, average accelerations were calculated based on slopes of vertical velocity vs. time curves. The maximum vertical acceleration of a spider would be 9.8 m s^{-2} if no forces act to slow down the spider. Air drag was estimated to cause deceleration of 0.5 m s^{-2} by filming a falling spider without a safety line, and for this reason drag was considered negligible compared to other uncertainties associated with the experiment. Therefore, any acceleration on the part of the spider that was substantially less than 9.0 m s^{-2} was considered to be result of additional friction forces such as an internal and/or external brake. One body weight of friction force should reduce acceleration to zero, resulting in a spider falling at a constant velocity. Any additional force would result in the spider decelerating and therefore coming to a stop. The relationship between the force acting on the dragline (in spider body weights, F_{BW}) and acceleration (A) can be expressed as:

$$F_{BW} = \frac{g - A}{g} \qquad (3.2)$$

Where g is the acceleration due to gravity, 9.8 m s^{-2}

For falls in which the length of silk did not change, or changed very little, silk tension could be approximated by treating the spider and silk as a pendulum. Total tension can therefore be considered the sum of the centripetal force Mgv^2l^{-1} and the vertical component of the spider's weight, $Mgcos\phi$. When expressed in body weights, the tension F_{BW}

$$F_{BW} = \frac{Mgv^2l^{-1} + Mg\cos\phi}{Mg} = v^2l^{-1} + \cos\phi \qquad (3.3)$$

depends on the velocity (v), length of silk (l), and the angle of the silk to the horizontal (ϕ) (see also Figure 3.11a).

Every fall consisted of periods in which silk length did not change followed by the spider spooling more silk. To calculate forces, therefore, each fall was separated into a vertical fall and pendulum motion and equation 3.2 or 3.3 used on each section.

Results

Friction Brakes

Silking anaesthetised spiders

There was no statistical difference between the 9 spiders silked at 0.02 m s^{-1} and 0.002 m s^{-1} (two-tailed t-test, $P = 0.367$), nor was there a statistically significant trend with spider mass (least squares regression, $r^2 = 0.0009$, $P = 0.91$). The average force was 0.76 ± 0.35 (sd) body weights. There was considerably more variability between individuals than for each spider in the response to silking in CO_2. One spider died during CO_2 exposure, but was silked anyway a number of times at both speeds, and the average resistance to silking was 0.20 ± 0.17 (sd) body weights of force.

Rear legs as friction brakes

Figure 3.2 shows a sample response from a spider with one leg free to grab the dragline as it is being silked. This spider repeatedly let go of the silk, giving a clear indication of how much force a single leg can apply. Overall, the response of spiders to silking with one leg holding the dragline was as variable as the previous experiment. Figure 3.3 shows the averaged forces attributed to the leg, as well as maximum and minimum transient forces. All spiders were capable of applying at least 1

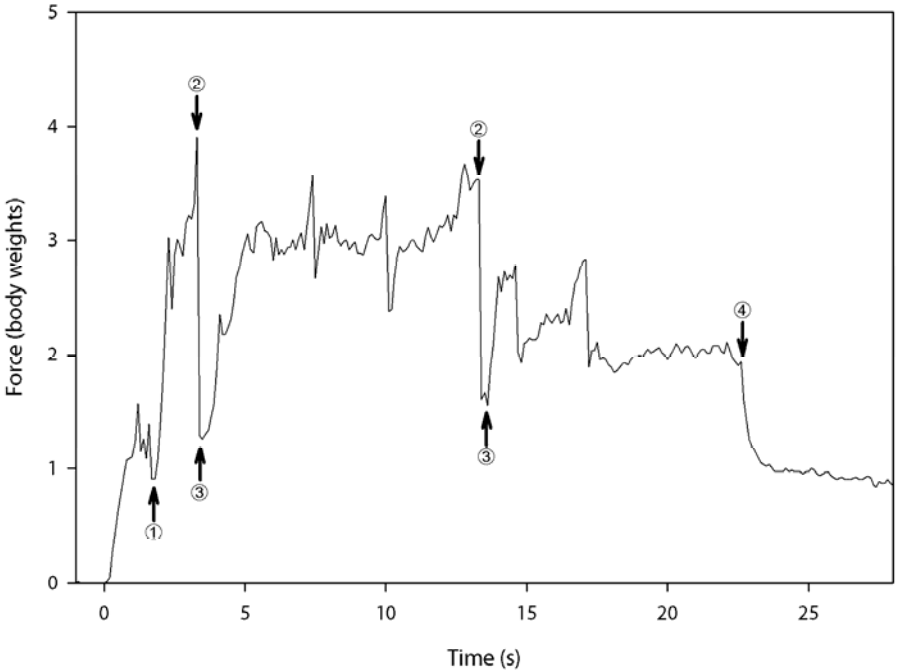

Figure 3.2 Sample data from a spider with one rear leg free to hold the dragline as it is being silked at 0.02 m s^{-1}. After the motor started at t = 0 seconds, silk was pulled through the leg's grip until ① when silk started being spooled out by the spider. At ②, the spider released the silk with its legs and grabbed it again at ③, so the difference represents the leg's contribution to the resisting force. The motor was turned off at ④.

body weight of force, and would therefore be able to decelerate with just one rear leg holding the silk. Transient forces were included because even short term forces can potentially overload and break a safety line if they are strong enough. All the measured friction forces were well below the breaking force predicted from equation 2.13 in the previous chapter, and the difference between maximum force and breaking force is the dynamic safety factor. Although there was no difference in friction forces applied by

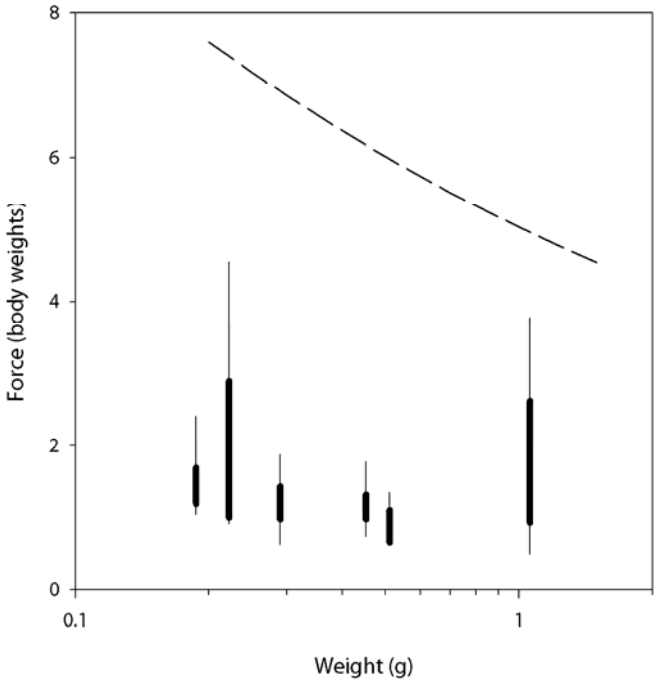

Figure 3.3 Summary of the spiders' ability to apply force to dragline with one rear leg while being silked. The thick lines represents the range of forces calculated from averaged data. The thin lines indicates the transient maximum and minimum forces that occurred within the averaged data. These were included because such transient forces could be enough to overload the silk and cause it to fail in use. The dashed line is the estimated breaking force in body weights of the silk ($F_{MAX, BW}$) from equation 2.13 in chapter 2.

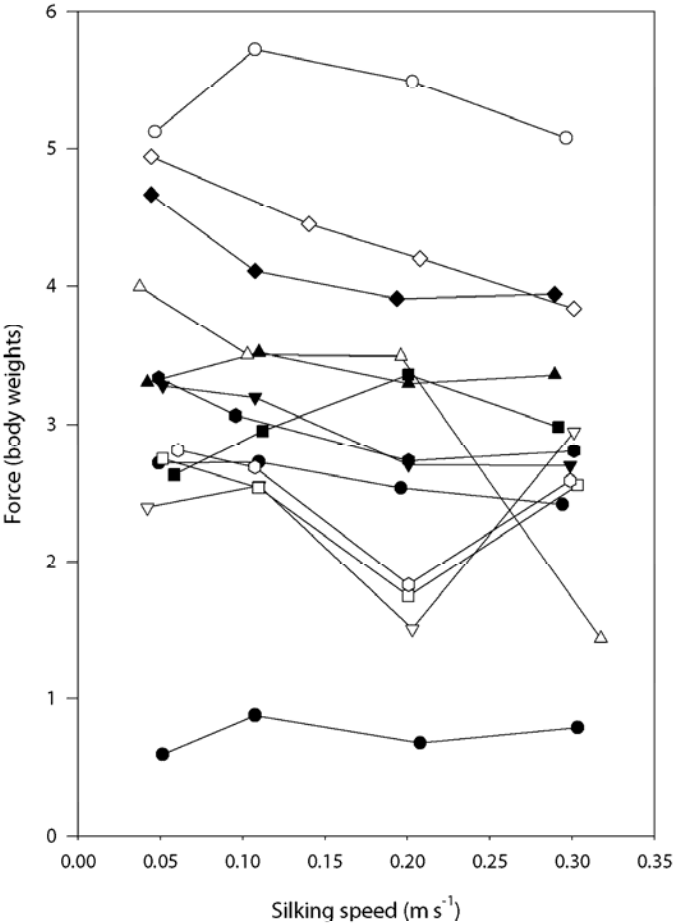

Figure 3.4 The spider's silking forces for each of four treatments. Each set of symbols represents one individual spider. Note that the silking force variation for each spider was much lower than the variation seen between different spiders.

the range of spiders, the large spiders have a lower working safety factor simply because the breaking force is lower

Internal friction brakes

Figure 3.4 shows the average force (F_{BW}) with which the 13 spider resisted being silked. While most of the spiders showed little difference between the different speeds, overall there was great variability between the spiders - the silking forces range form 0.6 to 5.7 body weights. To reduce this variation between individuals, force was normalized by dividing the average of each treatment by the overall average for that spider to give a unitless measure of silking force trends (see Figure 3.5). There is a significant correlation with a very low slope between normalized force and silking speed (least squares regression, P = 0.008) indicating that silking forces decline slightly with higher silking speeds. Figure 3.6 shows that the silking force (F) actually increases with spider mass when the force for each spider was averaged over the treatments. When expressed in body weights (F_{BW}), however, it is clear that silking friction force does not increase as rapidly as spider mass (Figure 3.7) so friction force declines with mass. The decrease in silking force is similar to the reduction in the silk's breaking force in body weights, and the two trends appear to be almost parallel. The difference between silking force and predicted breaking force is the dynamic safety factor. Note that this predicted dynamic safety factor increases from 3 to 4 with spider mass, but is applicable to tethered spiders being silked.

The data were also sorted by time to determine if spiders changed their response as a result of repeated silking. Since these data were normally distributed (P = 0.055), a One Way Repeated Measures anova was applied which confirmed that there were no statistical differences between the silking speeds (P = 0.16) as a result of repeated treatments or the spiders anticipating the motor being turned on.

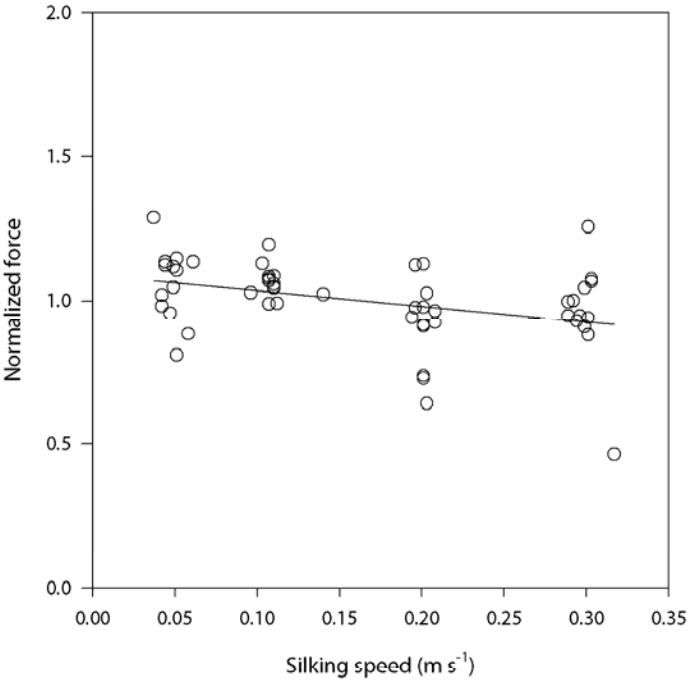

Figure 3.5 Normalized silking forces for different silking speeds. Because of the variation in the spider's response to being silked, silking force was nor-malized by dividing the average for each treatment by the overall average for that spider. The regression through the combined data from all 13 spiders is F_N = -0.0054v+1.09 (r^2= 0.132, P= 0.008) where F_N is the normalized force and v is silking speed.

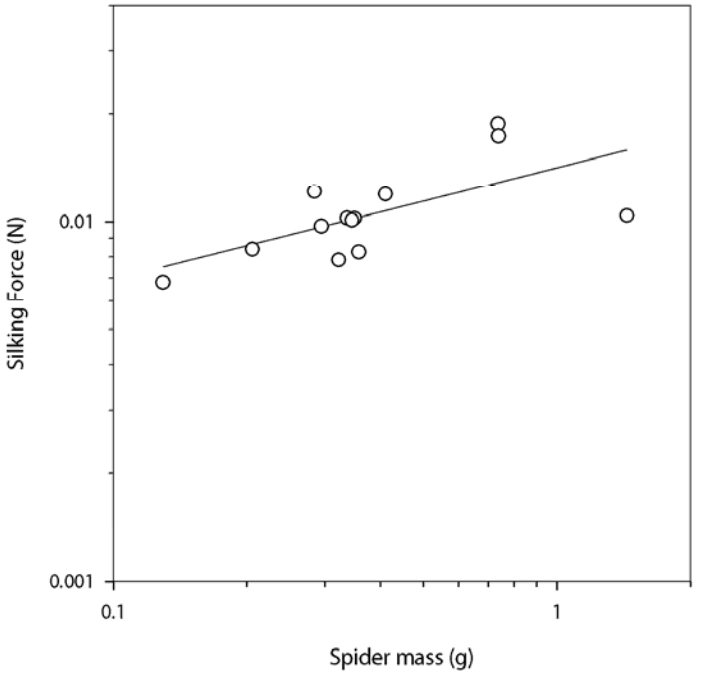

Figure 3.6 Average silking force in Newtons against spider mass. As spiders get heavier, silking forces increase in a statistically significant relationship $F = 1.42M^{0.31}$ ($r^2 = 0.42$, $P = 0.017$). Both axes were log transformed to fulfil the normality and constant variance assumptions of a regression analysis.

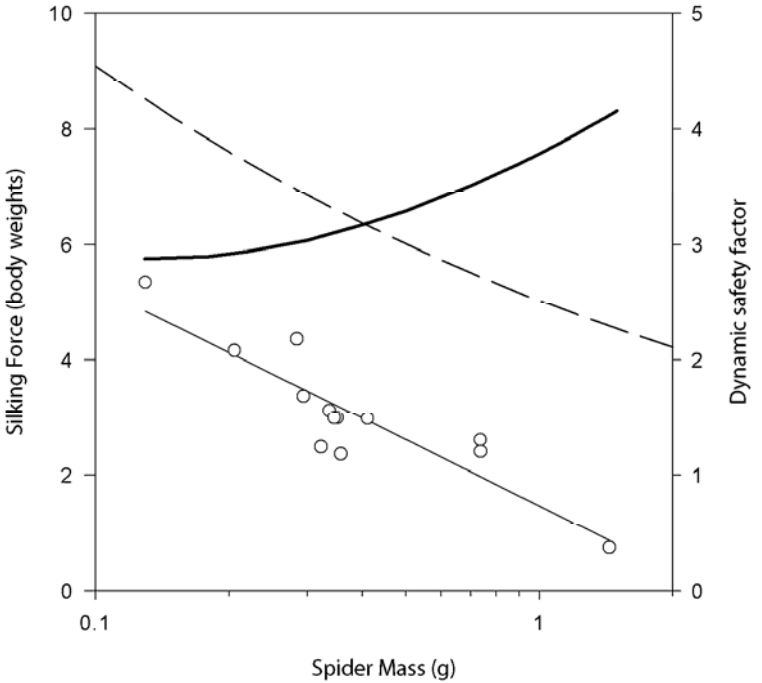

Figure 3.7 Silking force correlates strongly with spider mass, which was log transformed to maintain a normal distribution. The least squares regression of silking force in body weights (——), $F_{BW} = 1.05 - 4.79\log M$ ($r^2 = 0.80$) with respect to body mass M, has a slope significantly different from zero ($P < 0.0001$). The dashed line is the estimated breaking force in body weights of the silk ($F_{MAX,BW}$) from equation 2.13 in chapter 2. Also shown is the difference between the friction force regression and the predicted breaking force on the right axis as the dynamic safety factor (——)

The video record of the silking trials did not reveal any spinneret movement that could be associated with changes in silking forces. There were a number of common movements such closing the spinnerets in response to repeated stimulation, and a scrubbing motion in which the pairs of spinneret were rubbed against each other. This behaviour appeared to be a response to dragline getting caught in the spigots and setae, and resulted in a decrease in silking force. This suggests that dragline can get caught in the spigots and setae on the spinneret, but it is more of an accident than an intentional tension gate for applying friction to a dragline.

Silking to failure of silk

Sample data from each silking speed are presented in Figure 3.8. As most tests took over 60 seconds to complete, silking forces should only be considered approximations. Figure 3.9 shows that the slower the spider was silked, the longer the silk took to break or run out. Not surprisingly, longer silking times resulted in greater silk length and more silk mass per body weight, but the correlation with speed is not statistically significant.

All of these spiders had dragline that broke between the spinnerets and the motor spool, so dragline precursor had not been exhausted. All spiders except for one produced dragline immediately following the experiments, and only that spider did not produce dragline in the 4 days the spider remained under observation following the experiment. In all trials that lasted for more than a minute, the silk became visibly thinner, but no measurements were made.

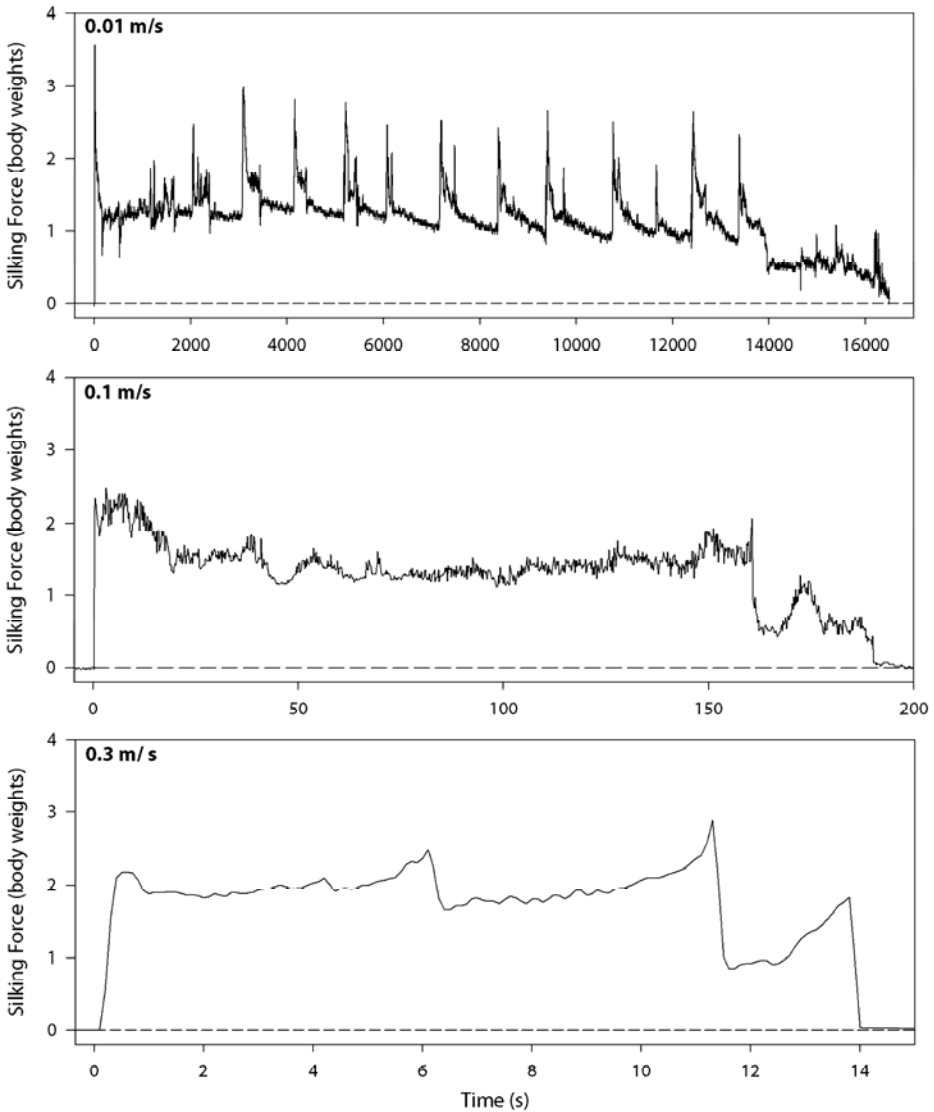

Figure 3.8 Sample graphs from spiders being silked dry at one of three speeds as indicated in the upper left hand corner of each graph. Note that the spider in figure 6a increased the silking force by more than one body weight every 16.9 ± 2.8 (sd) minutes. Because of transducer drift due to temperature and light fluctuations, the force records for experiments with more than 60 seconds between baselines can only be considered approximations. The spiders weighed 0.408 g, 0.600 g, and 0.723 g respectively.

A wide range of behaviours was observed. They ranged from controlled descents at constant low speeds, to bungee jumps when the spider fell with a premade length of silk. Spiders often went into a period of near-freefall after jumping or falling off, and decelerated after a short period. In no case did the silk break, although the attachment between silk and glass failed in two cases, both *A. diadematus*.

Spiders fell in such a way that all or portions of the fall could be classified as either vertical fall or pendulum-like. In a vertical fall, silk is spooled out and only a friction brake prevents the spider from reaching terminal velocity. A rapid change in velocity must be the result of the activation of a friction brake. Figure 3.10 shows a simple vertical fall by a *S. scenicus* in which forces can be easily calculated from

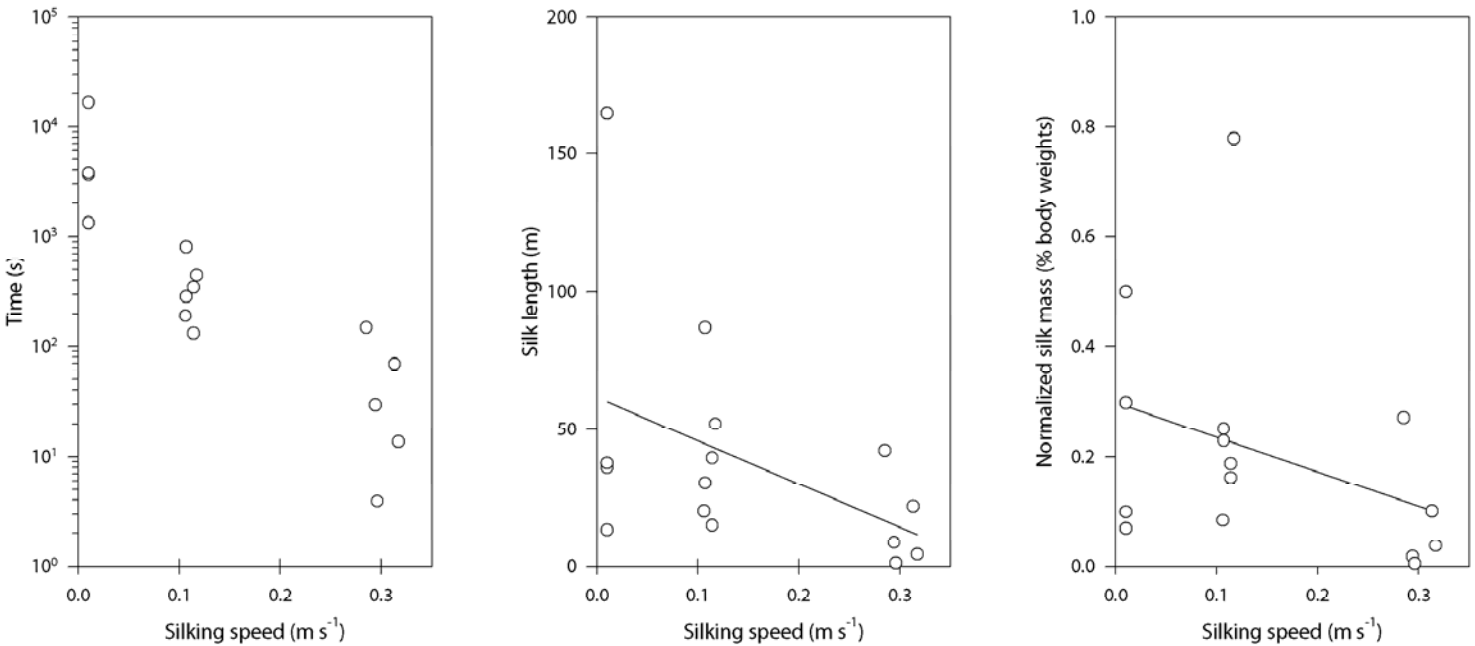

Figure 3.9 Summary of time to failure, silk length and normalized silk mass for spiders that were silked dry at one of three speeds. Note the time is shown on a log scale. The slower the spiders were silked, the longer it took for silk to run out or break. Similarly, longer silking time corresponded with greater length of silk obtained. There was no statistically significant trend between silk length and silking speed ($r^2 = 0.21$, $P = 0.08$) or normalized silk mass and silking speed ($r^2 = 0.14$, $P = 0.18$).

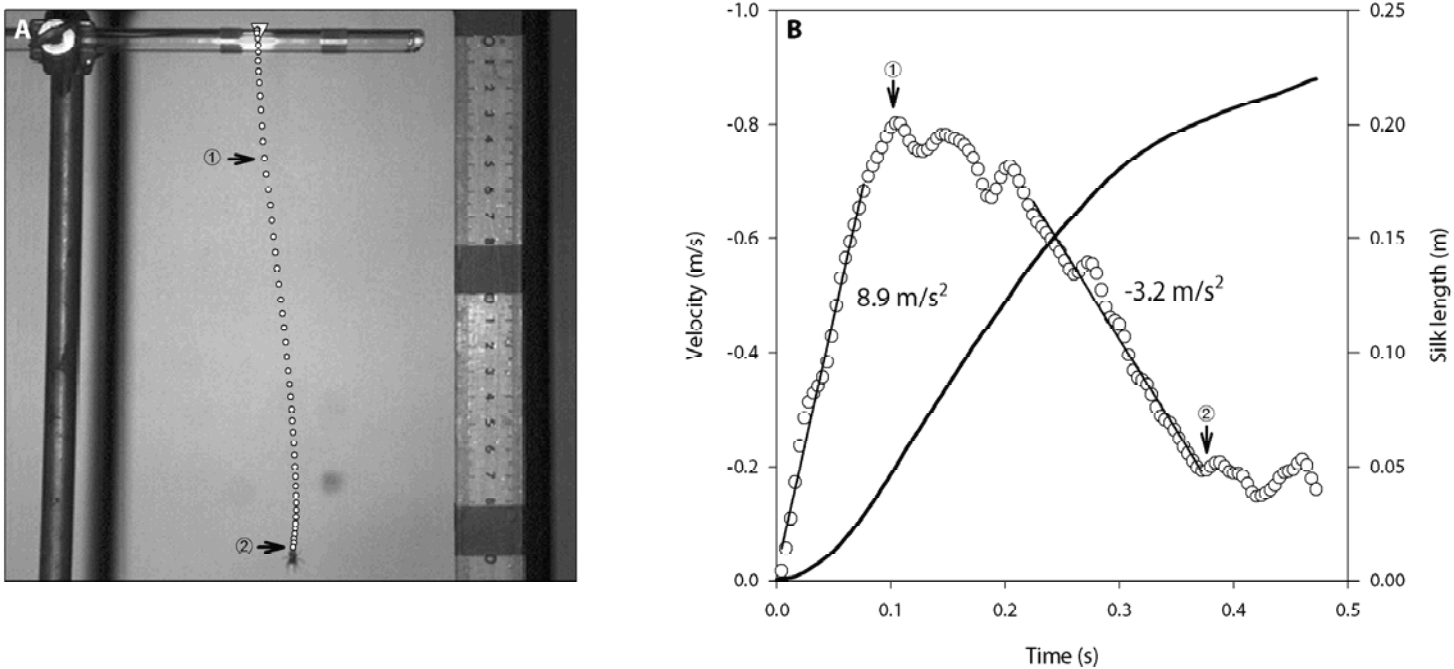

Figure 3.10 A typical vertical fall by a spider on its safety line filmed at 250 frames per second. Panel **A** is a composite of the x-y coordinates of the spider's centre of gravity from every second video frame, superimposed over the spider hanging from its dragline towards the end of the fall. The ruler is shown to the right of the spider, and the silk attachment point is marked by a white triangle (▽). At ① it started to decelerate by applying friction brakes, and it decelerated until ②, after which is continues to descend at a constant controlled speed beyond the view of the camera. Panel **B** shows the velocity (○) and silk length (——) calculated from the filtered data. Acceleration was calculated from least squares regressions (—) on the linear portions the velocity-time data and are reported beside the regressions.

the linear portions of the velocity-time data. The silk length increased during the entire fall, and the spider did not come to a stop until it hit the ground, although a brake was activated after 0.1 seconds, giving a breaking force of 1.3 body weights according to equation 3.1.

In a pendulum-like fall, little or no additional silk is spooled by the spider and so the force applied by the friction brakes must equal or exceed the tension in the dragline during the swing. Figure 3.11 illustrates a pendulum-like fall by a large *A. diadematus* as it loses it's grip on the glass rod and swings back and forth. The combination of centrifugal force and

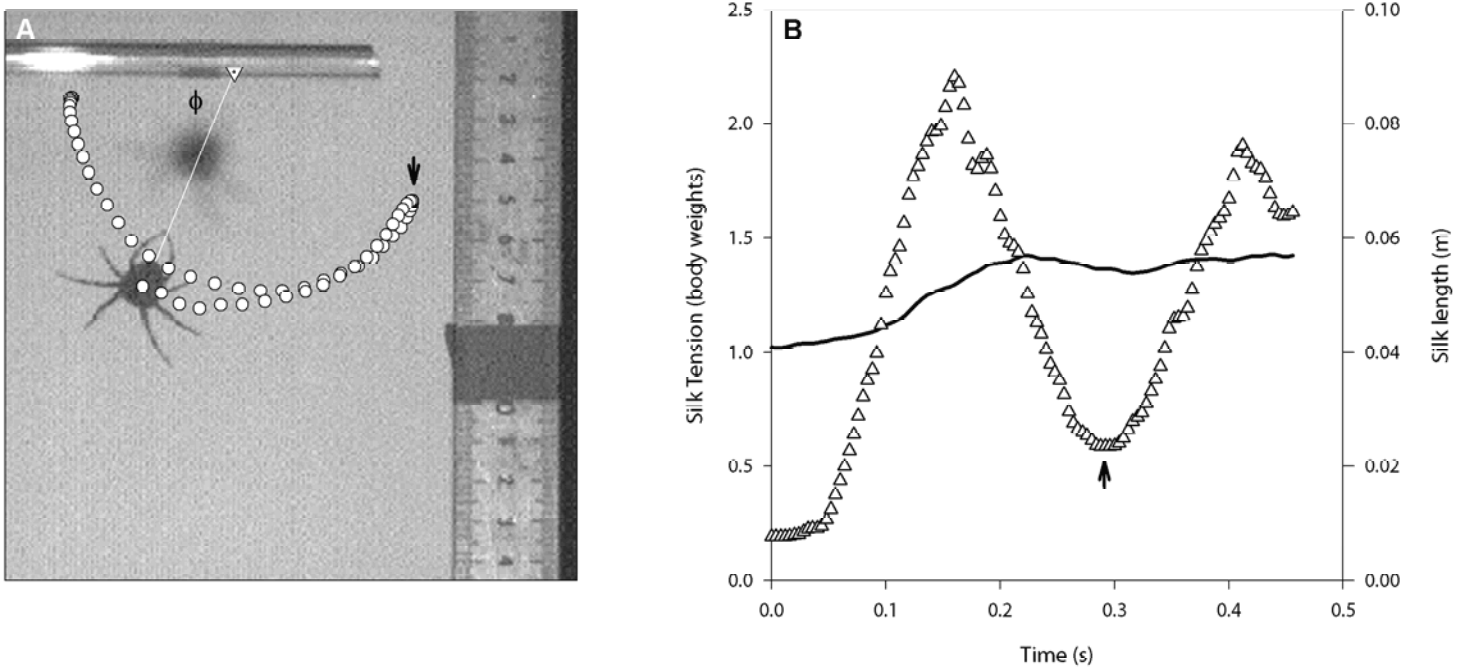

Figure 3.11 A typical pendulum-like fall where almost no additional silk is spooled by the spider, here a 0.76 g *A. diadematus*. Panel **A** is a composite of the x-y coordinates of the spider's centre of gravity from every video frame, super-imposed over the spider supporting itself on the end of its safety line. The silk attachment point is marked by a white triangle (▽). The spider started falling with a 4.1 cm length of dragline and swung towards the right. Note that both rear legs are holding the dragline by the end of the fall. The arrow in both panels shows where the direction of swing reversed. Panel **B** shows the resisting force in spider body weights (△) and silk length (—) calculated from the filtered data. Force is derived from equation 3.3 which calculates tension in a pendulum support.

spider weight peak at 2.3 body weights of force at the bottom of the pendulum arc.

A more complex fall is illustrated in Figure 3.12, where approximate silk tensions and friction forces are calculated separately for each section. It is interesting to note that the spider did not start spooling additional silk until silk tensions exceeded 1.5 body weights, but a friction brake of 2.4 body weights is applied shortly after to bring the spider to a stop. Note that peak vertical velocity of silk production was 1.3 m s^{-1}, much faster than the 0.3 m s^{-1} at which spiders could be consistently silked at by the experimenter.

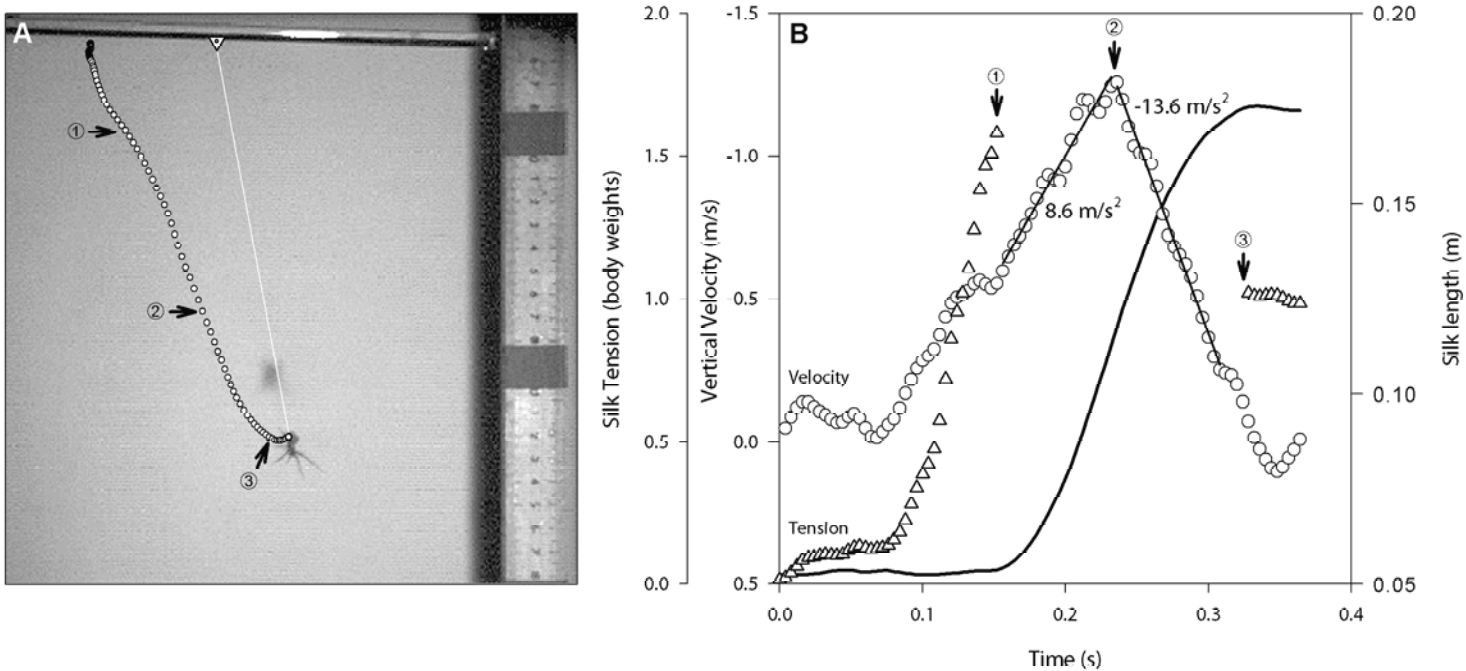

Figure 3.12 An example of a fall with alternating periods of silk spooling and constant silk length by a 0.076 g male *A. diadematus* spider. The spider had attached silk (▽) and walked 5.3 cm before losing its grip. Panel a is a composite of the x-y coordinates of the spider's centre of gravity from each video frame, superimposed over the spider hanging from its dragline at the end of the fall. Once the spider falls, the silk length is constant until the spider starts spooling more silk at ①. From the rapid change in velocity, it is apparent that friction brakes are engaged at ②, decelerating the spider until it stops spooling silk at ③. Panel b shows silk tension (△) calculated for the sections of the fall where silk length remained essentially unchanged (before ①, after ③), and vertical velocity (○) against time. While the spider was dropping vertically while spooling silk from ② to ③, forces were estimated by determining accelerations from linear portions of the velocity-time data and are reported beside the regressions. As the rear legs were apparently not in contact with the dragline, all change in velocity must be due to the spider's internal friction brakes.

Figure 3.13 summarizes the range of friction forces calculated for the 3 *S. scenicus* and 8 *A. diadematus* spiders from pendulum–like and vertical falls. All the jumping spiders show negative friction forces on at least one occasion which is only possible by actively jumping off of the glass rod as opposed to falling. Except for the tendency of jumping spiders to jump, both species show similar ranges of applied friction forces and no apparent trend with spider mass. When the generated friction forces are compared to predicted breaking forces in body weights of the silk ($F_{MAX,\ BW}$) from equation 2.13, we can see that while applied friction forces for *A. diadematus* do not come close to predicted failure forces, *S. scenicus* maximum friction forces fall right on its predicted failure points.

The dynamic safety factor, calculated as the ratio of predicted failure forces to the maximum friction forces in Figure 3.13 is shown in more detail in Figure 3.14. As with any other safety factor, values less than 1 mean that the structure is too weak and will break in use. *A. diadematus* dynamic safety factor declined with spider mass, to a minimum of 2 for the very largest individual. The *S. scenicus*, on the other hand,

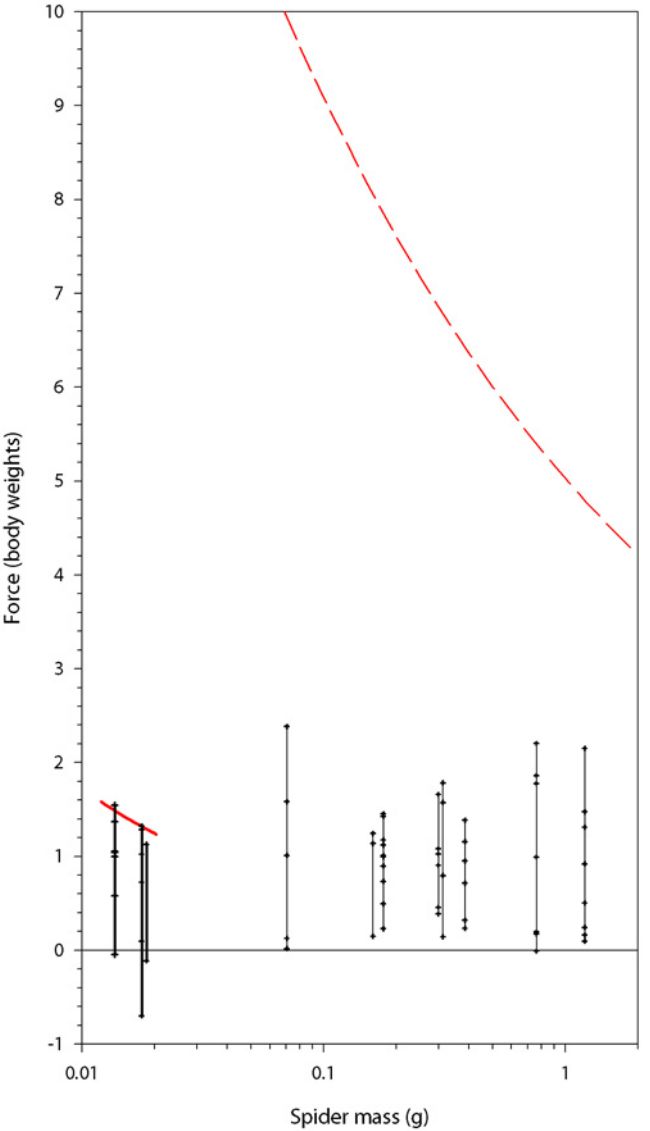

Figure 3.13 Summary of silk forces in falling spiders. The graph shows data from falls by 3 adult *S. scenicus* (—) and 8 adult *A. diadematus* (–), where each line represents the range of forces calculated from one or more falls for that spider. Each point on the line represents one period of acceleration calculated from a vertical velocity regression, or the maximum and minimum tensions in a pendulum swing. Note that the range of accelerations is similar between species as well as over the 200 fold weight range of *A. diadematus*, although *S. scenicus* includes negative forces which is only possible if the spiders actively jumped down. Also shown are the estimated breaking force in body weights of the silk ($F_{MAX,\ BW}$) from equation 2.13 in chapter 2 for *A. diadematus* (- - -) and *S. scenicus* (—).

had working safety factors slightly above or below 1 and are therefore stressing their dragline to its fullest capabilities when using their friction brakes naturally.

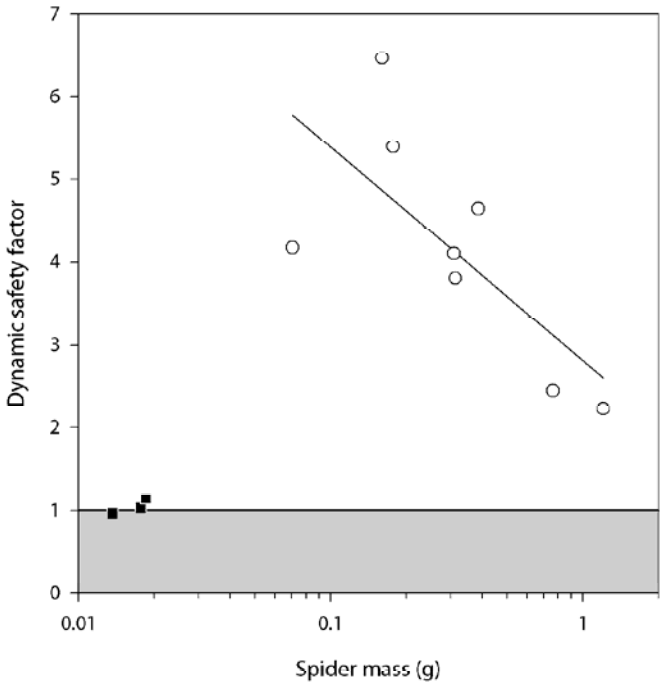

Figure 3.14 The dynamic safety factor for *A. diadematus* (○) declines with spider mass, while *S. scenicus* (■) has a working safety factor that hovers around 1. The shaded area represents safety factors less than 1, where the dragline should break. Note that one *S. scenicus* falls into this area although its silk did not in fact fail. The least squares regression equation of dynamic safety factor (S_F) against spider mass (M) is $S_F = 2.82 - 2.572\log M$ ($r^2 = 0.96$, $P < 0.0001$) is shown as a solid black line.

Discussion

As the video analysis presented in this study clearly shows, spiders do not bungee jump because they spool out more silk as they fall. This gives them the opportunity to dissipate kinetic energy by converting it to heat through the use of one or more friction brakes. Together with other sources of friction, such as air drag, these brakes determine the acceleration of the falling spider. If a total of one body weight of friction force is applied, the spider will fall at a constant velocity. If the friction is greater than one body weight, the spider will decelerate and eventually come to a stop.

Work (1978) proposed that the spinnerets could function as a friction brake by forcing silk to run under and over setae and spigots, with the position of the spinnerets controlling the complexity (and friction) of the silk's path. The video recording made during silking showed that while the silk rarely ran free of the spinnerets after emerging from the anterior spigots, no spinneret movements were observed that corresponded with changes in recorded frictional silk to friction. It is therefore unlikely that this is a commonly used friction brake in spiders.

A single rear leg, on the other hand, is a very capable tension gate. It can apply 0.7 to 3 body weights of force which is to decelerate or support a spider on its dragline, especially since both rear legs can be used simultaneously. Under natural conditions, *A. diadematus* can be seen using its rear leg friction brake frequently. Most commonly, it is used when the spider comes to a stop, and then supports its weight with one or more legs. Also, slow descents are often made with one leg holding the dragline. During rapid escape

type manoeuvres, however, the legs are generally held out to the side as the spider falls, and rapid decelerations are also generally performed without using the legs. This suggests that leg friction brakes are more suitable for maintained forces rather sudden stop and starts.

From Wilson (1962a) we know that only the orb-weavers appear to have valves between the lumen of the silk gland and the spigot, while other spiders have only nodes. This suggests that the valve does not function as a friction brake because other spiders, such as the jumping spiders studied here, are fully capable of decelerating on a dragline without the use of their rear legs. Another more common structure must act as a friction brake, and I propose that it is in fact the duct levator muscle, which runs from beside the spigot to just past the valve (or node) and is present in all spiders that were examined by Wilson (see Figure 3.15). When this muscle contracts, it is likely that the normally straight duct is bent into an *S* curve, causing silk to rub along the sides of the duct. It has been observed by Wilson (1962a) that this section of the duct is frequently bent in preserved specimen.

Vollrath and Knight (1999) proposed that the combination of valve, valve tensor muscle and duct levator muscle could act as a ratchet to restart silk that had broken off in the duct, and this would not be inconsistent with the possibility that the duct levator muscle can act as the friction brake. Restarting silk is, however, unlikely to be a problem unique to orb weavers, and so probably involves structures common to all spiders.

Silk separates from the duct anterior to the valve/node and

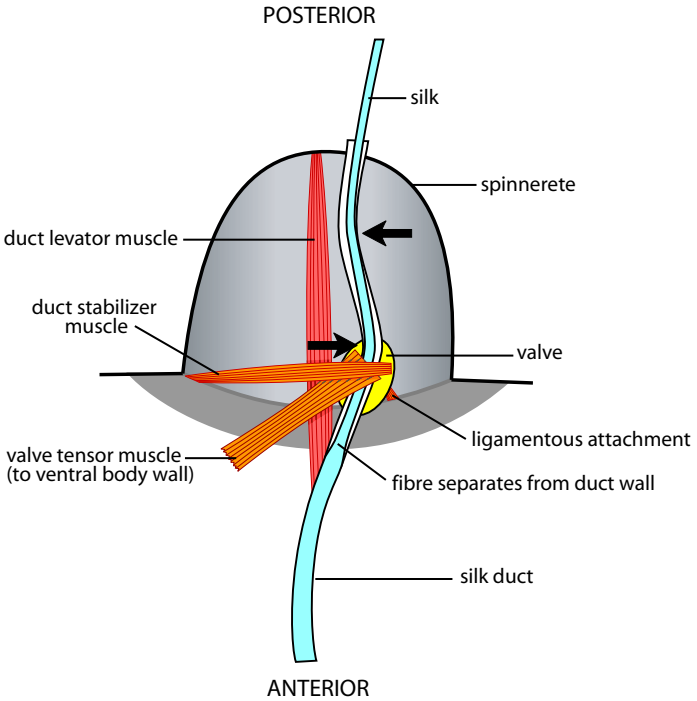

Figure 3.15 Cross-section throught the anterior spinneret of *A. diademtus* showing the major ampullate silk duct and its associated muscles. The cuticular lining of the duct was omitted. The duct levator muscle is shown slightly contracted, which could result in a curvature to the silk duct. Arrows indicate sources of friction as silk comes in contact with the duct walls. Adapted from Wilson, 1962a.

so is solid from that point on (see Figure 3.15). The process of drawing out the silk requires force which I attempted to quantify by silking anaesthetised spiders. The measured force of 0.76 body weights appears to be too high as spiders falling normally frequently applied less force than that (see

Figure 3.14), but the 0.2 body weights of force measured on a dead spider may be closer. It is possible that CO_2 anaesthetisation altered the acid-base balance in the spiders resulting in an abnormal response.

Dissipating energy as friction reduces the impact load on the silk, but does produce heat. A simple estimate can be made of the heat generated. The product of force (N) and speed (m s^{-1}) is power (J s^{-1}), so a 0.1 gram spider applying 2 body weights of force while falling at 1.3 m s^{-1} (see Figure 3.12) would be producing 2.6×10^{-3} J s^{-1}. Given that it takes 4.2 J to raise the temperature of 1 gram of water by 1 °C, the rate of heating for the entire spider is approximately 0.006 °C s^{-1}. It is more likely, however, that the heat is concentrated around the friction brake, so if that represents 1% of body weight, localized heating would be on the order of 0.6 °C s^{-1}. This could quickly cause damage, but under normal conditions spiders don't apply these brakes for long, especially not at those speeds.

Heat build-up in the duct and surrounding tissues could be a potential problem for a spider decelerating for an extended period of time. Falling spiders did not apply friction brakes to spooling silk for more than 10 seconds, either coming to a stop or ending up on the ground. During extended period of forced silking, damage to surrounding tissues is a possibility, however, no trend indicating less silk with faster silking was observed when spiders were silked at different speeds until the silk gave out. Higher speeds should have resulted in more friction and therefore more heat. While the spiders being silked at high speeds ran out of silk or cast it off much earlier than spider silked at slower speeds, the mass of silk collected per body weight was statistically the same as at other speeds. Friction induced heating may, however, explain why spiders could not be silked consistently at speeds exceeding 0.3 m s^{-1} especially since smaller spiders applied more force relative to their body weight.

To bring the spider to a stop, any friction force over one body weight is enough. Clearly, either of the friction brakes discussed is more than sufficient for that purpose. The video analysis showed *A. diadematus* rarely used more than 2 body weights of force when falling, and the most that the jumping spider, *S. scenicus*, used was 1.6. In fact, *S. scenicus* loaded its dragline almost to the failure point, resulting in a dynamic safety factor of 1. The dynamic safety factor for *A. diadematus*, on the other hand, started at 6 and declined to 2.5 as spider mass increased.

The most likely explanation for why *A. diadematus* dragline appears overbuilt in comparison to *S. scenicus* is that jumping spiders do not build webs. In fact, jumping spiders use dragline only as a safety line, and it appears to be well matched to its function in that 1.6 body weights of force are more that adequate to bring the spiders to a rapid stop with a carefully controlled friction brake even though the dynamic safety factor is 1. Orb weavers, however, also build webs using dragline, so the higher dynamic safety factors most likely reflect this additional design requirement

One other observation can be made about the data. None of the spiders of either species broke their dragline during any of the recorded falls, although two attachment disks failed. This is despite the fact that working safety factors for

S. scenicus approached 1. In light of the fact that Gorb and Barth (1996) found evidence of mechanosensory cells on the spinnerets of the wolf spider *Cupiennius salei*, it is likely that the spiders can sense how much their dragline is loaded. Anticipating when the dragline will fail and compensating by spooling additional silk would then only be a matter of learning. This would explain how *S. scenicus* can come so close to the load limit of their silk, but not break it.

This research may also be of interest to anyone silking spiders to measure material properties of the silk. The experiments showed that while any one spider was consistent in how it responded to being silked at various speeds, there is great variability in silking force between spiders. Furthermore, spiders silked for extended periods did not respond with uniform silking forces, but increased force for short periods in a very regular pattern. Because shear forces on the forming silk can affect material properties (Knight et al., 2000), variable forces between and within silk samples will greatly increase variability in material property data. In addition, silking forces recorded from forcibly silked spiders were consistently higher than what the spider applied to silk during a normal fall which may be artificially increasing measured silk strengths in some experiments.

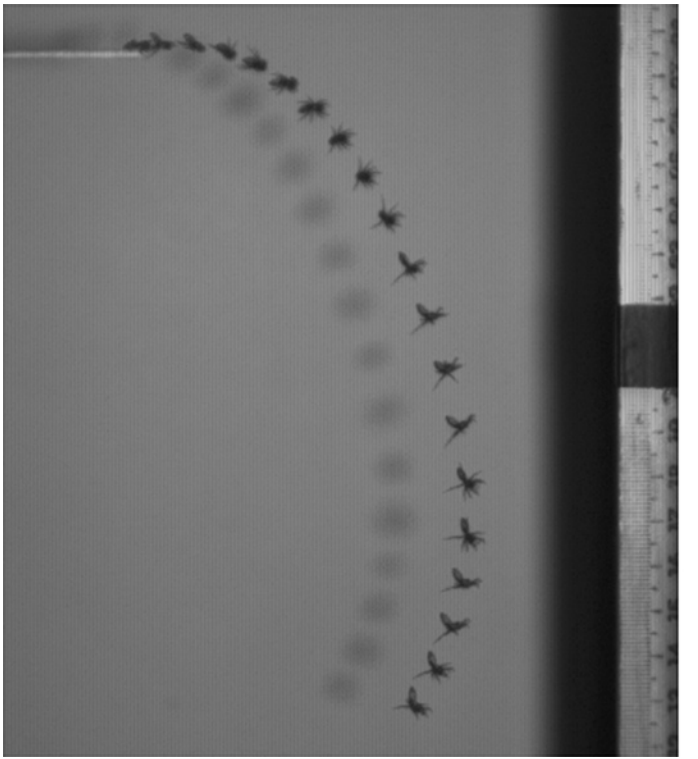

Space filler #2 ~ a jumping *Salticus scenicus* filmed at 250 Hz.
This this a composite image made up of every third frame.

Chapter 4: Conclusion

For reasons yet unknown, the relationship between spider mass and dragline breaking force is best described by a power function with a exponent of 0.74 for *A. diadematus*, and 0.54 for *S. scenicus*. The consequence of this is that the static safety factor of the dragline declines as the spiders get larger, the opposite of what would be expected is the scaling was driven by safety line design. One possible explanation is that small instars need proportionally stronger silk in order to catch prey. This is especially true for first and second instar *A. diadematus* which must build webs strong enough to capture prey larger than the spider, and to resist wind loading. The dragline for both species is too weak to survive a bungee jump with a fixed length of silk. Evaluating dragline as a safety line relative to the worst case scenario tells us that the silk is built to different standard.

Three sources of friction were investigated; the rear leg acting as a friction brake, an internal friction brake, and silk formation in the ducts. Both friction brakes can apply at least one body weight of force, enough to decelerate a falling spider. Maximum holding force of the internal brake depends on spider mass, while the rear leg's friction force did not appear to be correlated to spider mass. The most likely mechanism for the internal friction gate is the levator muscle contracting to bend the silk duct, causing friction between the solid silk and the sides of the duct. The valve is not likely involved as a clamp because it is only found in orb weaving spiders.

Film analysis of falling spider showed that under normal conditions the spiders do not apply more than 2.5 body weight of force. This corresponds to a working safety factor of 2 to 7 for *A. diadematus*, and 1 for *S. scenicus*. That *S. scenicus* stresses its silk to such an extent is circumstantial evidence that the mechanosensory receptors located near the dragline spigots act as force transducers.

Overall, the data support the idea that the dragline is a compromise between different constraints. The jumping spider *S. scenicus* , by being small, will not get hurt in a fall, and the cost of continuously laying down dragline as the spider moves must be minimized. This results in a dragline that is just barely capable of supporting the forces of falling spider as friction brakes to applied to its spooling silk. *Araneus diadematus*, on the other hand, build webs rather than actively hunting, and the gravid females are large enough to damage themselves in a fall. The need to build strong webs, while having a dragline that is safety to use for vertical locomotion and as a safety line, has led to a dragline which is stronger that what would be expected for a simple safety line.

There are a number of other experiments that arise from this thesis. Firstly, adult *S. scenicus* could be forcibly silked to characterize their friction brakes and determine if, like *A. diadematus*, the brakes are stronger than what is seen during a normal fall. And secondly, silking experiments could be performed to isolate the friction brake in *A. diadematus* and another large spider that does not have a valve. This would be achieved by electrically stimulating the duct levator muscle while forcibly silking anaesthetised spiders. This would separate the possible contributions to friction of the valve and duct levator muscle.

Bibliography

Alexander, R. McN. (1996). *Optima for Animals*, revised edition. pp. 24-25 Princeton, New Jersey: Princeton University Press.

Alexander, R. McN. (1981). Factors of safety in the structure of animals. *Scient. Prog. Oxford* **67**, 109–130.

Blockey, D. I. (1980). *The Nature of Structural Design and Safety*. Page 120. West Sussex, England: Elis Horwood Limited.

Brandwood, A. (1985). Mechanical properties and factors of safety of spider drag-lines. *J. exp. Biol.* **116**, 141-151.

Bristowe, W. S. (1931). A Preliminary note on the spiders of Krakatau. *Proc. Zool. Soc Lond*. **100,** 1387-1400.

Corning, W. S., and Biewener, A. A. (1998). *In vivo* stains in pigeon flight feather shafts: implications for structural design. *J. exp. Biol.* **206,** 3057-3065.

Cromptin, J. (1951). *The Life of the Spider*. Page 142. Boston, Massachusetts: Houghton Mifflin Company

Denny, M. (1976). The physical properties of spider's silk and their role in the design of orb-webs. *J. Exp. Biol*. **65,** 483-506.

Foelix, R. F. (1996). *Biology of Spiders*, second edition. New York, New York: Oxford University Press Inc.

Gorb, S. N., and Barth, F. G. (1996). A new mechanosensory organ on the anterior spinnerets of the spider *Cupiennius salei* (Araneae, Ctenidae). *Zoomorphol.* **116,** 7-14.

Gorb, S. N., Landolfa, M. A., and Barth, F. G. (1998). Dragline-associated behaviour of the orb-web spider *Nephila clavipes* (Aranoidea, Tetragrathidae) *J. Zool. Lond.* **244,** 323-330.

Gosline, J. M., DeMont, M. E., and Denny, M. (1986). The structure and properties of spider silk. *Endevour* **10,** 37-43.

Gosline, J. M., Guerette, P. A., Ortlepp, C. S., and Savage, K. N. (1999). The mechanical design of spider silks: from fibroin sequence to mechanical function. *J. Exp Biol*. **202,** 3295-3303.

Hallas, S.E.A., and Jackson, R.R. (1986). Prey-holding abilities of the nests and webs of jumping spiders Araneae Salticidae. *Journal of Natural History* **20,** 881-894.

Jackson, R. R., and Wilcox, R. S. (1998). Spider-eating spiders. *American Scientist*. **86,** 350-357.

Kirkpatrick, S. J. (1994). Scale effects on the stresses and safety factors in the wing bones of birds and bats. *J. exp. Biol.* **190,** 195-215.

Knight, D. P., Knight, M. M., and Vollrath F. (2000). Beta transition and stress-induced phase separation in the spinning of spider silk. *Int. J. Biol. Macromol.* **27,** 205-210.

Köhler, T., and Vollrath, F. (1995). Thread biomechanics in the two orb-weaving spiders *Araneus diadematus* (Araneae, Araneidae) and *Uloborus walckenaerius* (Araneae, Uloboridae). *J. Exp. Zool*. **271,** 1-17.

Lucas, F. (1964). Spiders and their silks. *Discovery, Lond.* **24,** 20-26.

Osaki, S. (1996). Spider silk as mechanical lifeline. *Nature* **384,** 419.

Pollak, C. C. (1991). Mechanical and optical analysis provide a network model for spiral silk from the orb web of the spider *Araneus diadematus*, Masters thesis. University of British Columbia, B.C.

Prange, H. D. (1977). The scaling and mechanics of arthropod exoskeletons. In Pedley, T. J., ed.: *Scale Effects in Animal Locomotion*, pp 169-181. London: Academic Press.

Robinson, M. H., and Valerio, C. E. (1977). Attacks on large or heavily defended prey by tropical salticid spiders. *Psyche* **84,** 1-10.

Shelden, P. A., Shear, W. A., and Bonamo, P. M. (1991). A spider an other arachnids from the Devonian of New York, and reinterpretation of Devonian Araneae. *Paleontology* **34,** 241-250.

Smith R. B., and Mommsen, T. P. (1984). Pollen feeding in an orb-weaving spider. *Science*, **226,**1330-1332.

Stauffer, S., Coguill, S. L., and Lewis, R. V. (1994). Comparison of physical properties of three silks from *Nephila clavipes* and *Araneus gemmoides*. *J. Arachnol* **22,** 5-11.

Tietjen, W.J., and Rovner, R.S. (1980) Physico-chemical trail-following behaviour in two species of wolf spiders: sensory and etho-ecological concomitants. *Anim. Behav*. **28,** 735-741.

Tietjen, W.J., and Rovner, R.S. (1982). Chemical communication in Lycosida and other spiders. In: Will, P.N., Rovner, J.S., ed.: *Spider Communication. Mechanisms and Ecological Significance*. Princeton, New Jersey: Princeton University Press. pp 249-278

Vogel, S. (1994). *Life in Moving Fluids, the physical biology of flow*, second edition. Page 335. Princeton, New Jersey: Princeton University Press

Vollrath, F., and Köhler, T. (1996). Mechanics of silk produced by loaded spiders, *Proc. R. Soc. Lond. B*, **263,** 387-391.

Vollrath, F., and Knight, D. P. (1999). Structure and function of the silk production pathway in the spider *Nephila edulis*. *Int. J. Biol. Macromol.* **24,** 243-249.

Williams, D. S., and McIntyre, P. (1980). The principal eyes of a jumping spider have a telephoto component. *Nature*. **288,** 578-560.

Wilson, R. S. (1962a). The structure of the dragline control valves in the garden spider. *Quart. J. Micr. Sci.* **103,** 549-555.

Wilson, R. S. (1962b). The control of the dragline spinning in the garden spider. *Quart. J. Micr. Sci.* **104,** 557.

Winter, D. A. (1990). *Biomechanics and the control of human movement*, second edition. New York, New York: Wiley-Interscience Publications

Witt, P., Reed, C. F., and Peakall, D. B. (1968). *A spider's web - problems in regulatory biology*. pp 49-53. Springer Verlag, New York Inc.

Work, R. W. (1977). Mechanisms of major ampullate silk fiber formation by orb-web-spinning spiders. *Trans. Amer. Micros. Soc.* **92,** 170-189.

Work, R. W. (1978). Mechanisms for the deceleration and support of spiders on draglines. *Trans. Amer. Micros. Soc.* **97,** 180-191.

Work, R. W. (1981). A comparative study of the super-contraction of major ampullate silk fibers of orb-web-building spiders (Araneae). *J. Arachnol*. **9,** 299-308.

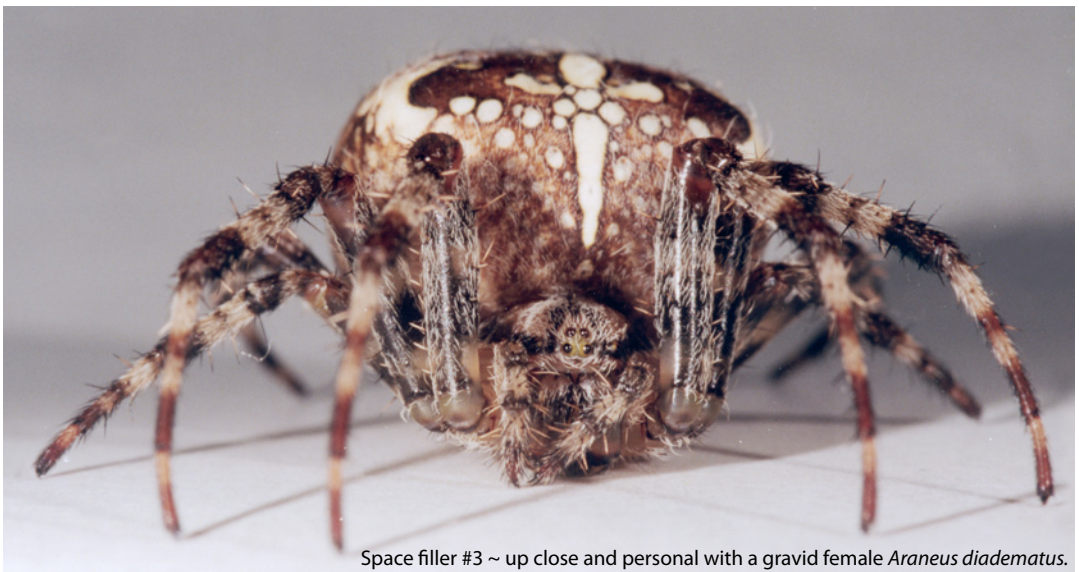

Space filler #3 ~ up close and personal with a gravid female *Araneus diadematus.*